Molecular Biology of the Cell
Vol. 19, 4224–4237, October 2008

Arf GTPase-activating Protein ASAP1 Interacts with Rab11 Effector FIP3 and Regulates Pericentrosomal Localization of Transferrin Receptor–positive Recycling Endosome

Hiroki Inoue,* Vi Luan Ha,* Rytis Prekeris,† and Paul A. Randazzo*

*Laboratory of Cellular and Molecular Biology, National Cancer Institute, National Institutes of Health, Bethesda, MD 20892; and †Department of Cellular and Developmental Biology, School of Medicine, University of Colorado Health Sciences Center, Denver, CO 80262

Submitted March 18, 2008; Revised July 18, 2008; Accepted July 25, 2008
Monitoring Editor: Jean E. Gruenberg

ADP-ribosylation factors (Arfs) and Arf GTPase-activating proteins (GAPs) are key regulators of membrane trafficking and the actin cytoskeleton. The Arf GAP ASAP1 contains an N-terminal BAR domain, which can induce membrane tubulation. Here, we report that the BAR domain of ASAP1 can also function as a protein binding site. Two-hybrid screening identified FIP3, which is a putative Arf6- and Rab11-effector, as a candidate ASAP1 BAR domain-binding protein. Both coimmunoprecipitation and in vitro pulldown assays confirmed that ASAP1 directly binds to FIP3 through its BAR domain. ASAP1 formed a ternary complex with Rab11 through FIP3. FIP3 binding to the BAR domain stimulated ASAP1 GAP activity against Arf1, but not Arf6. ASAP1 colocalized with FIP3 in the pericentrosomal endocytic recycling compartment. Depletion of ASAP1 or FIP3 by small interfering RNA changed the localization of transferrin receptor, which is a marker of the recycling endosome, in HeLa cells. The depletion also altered the trafficking of endocytosed transferrin. These results support the conclusion that ASAP1, like FIP3, functions as a component of the endocytic recycling compartment.

INTRODUCTION

Arf family GTP-binding proteins and their GTPase-activating proteins (Arf GAPs) play crucial roles for membrane traffic and actin remodeling (D'Souza-Schorey and Chavrier, 2006; Gillingham and Munro, 2007). Arf GAPs share the same catalytic domain, the Arf GAP domain, which is responsible for GTP hydrolysis. In humans, 31 genes encoding proteins with Arf GAP domains have been found. They are classified into several subfamilies based on their domain structures (Randazzo *et al.*, 2007; Inoue and Randazzo, 2007). Three subfamilies, ArfGAPs, SMAPs, and GITs, have an Arf GAP domain at the N-terminus of the molecules. In contrast, the others, which are called AZAP-family Arf GAPs, contain an Arf GAP domain following a pleckstrin homology (PH) domain in the middle of the protein. They are subdivided into four subfamilies, ASAPs, ACAPs, ARAPs, and AGAPs.

ASAP1 is one of the best-characterized Arf GAPs. In addition to PH and Arf GAP domains, ASAP1 contains an N-terminal Bin, Amphiphysin, and Rvs167/Rvs161 (BAR) domain and, in the C-terminal half of the protein, a proline (Pro)-rich domain and Src homology 3 (SH3) domain. Other ASAP isoforms, ASAP2 and ASAP3, have similar domain structures and high homology, especially in the Arf GAP domains, although ASAP3 lacks C-terminal SH3 domain (Ha *et al.*, 2008). Through its Pro-rich and SH3 domains, ASAP1 interacts with a number of proteins, which are mainly adhesion- and actin cytoskeleton–related proteins including Src, focal adhesion kinase (FAK), Crk/CrkL, and cortactin (Brown *et al.*, 1998; Liu *et al.*, 2002; Oda *et al.*, 2003; Onodera *et al.*, 2005; Bharti *et al.*, 2007). ASAP1 is a component of three integrated membrane/actin cytoskeleton structures: focal adhesions, circular dorsal ruffles (CDRs) and invadopodia/podosomes. ASAP1 associates with focal adhesions in fibroblasts (Randazzo *et al.*, 2000). The focal adhesion localization depends on the interaction of ASAP1 with FAK and CrkL (Liu *et al.*, 2002; Oda *et al.*, 2003). Altered ASAP1 expression reduces the paxillin content of focal adhesions. ASAP1 also associates with CDRs (Randazzo *et al.*, 2000). These structures, which are induced by growth factors such as platelet-derived growth factor (PDGF), are rings of dynamically remodeling polymerized actin at the dorsal surface of cells associated with plasma membranes undergoing extensive endocytosis. Recently, ASAP1 has been reported to localize with another class of membrane/actin structures called invadopodia and podosomes (Onodera *et al.*, 2005; Bharti *et al.*, 2007; Randazzo *et al.*, 2007). They are adhesive structures on the ventral surface of cells found in metastatic breast cancer cells and active Src-transformed fibroblasts and are thought to mediate cancer cell invasion into normal tissue (Buccione *et al.*, 2004). Depletion of ASAP1 in cells prevented formation of invadopodia and podosome structure, and, in some studies, reduced invasion. These findings support the idea that ASAP1 functions as a regulator of the actin cytoskeleton, which is involved in cell adhesion, migration and invasion.

BAR domains form crescent-shaped homodimers and are a membrane-binding module that induces or senses membrane curvature (Takei *et al.*, 1999; Lee *et al.*, 2002; Peter *et al.*, 2004). They are found in many proteins that are involved in

This article was published online ahead of print in *MBC in Press* (http://www.molbiolcell.org/cgi/doi/10.1091/mbc.E08–03–0290) on August 6, 2008.

Address correspondence to: Paul A. Randazzo (Randazzo@helix.nih.gov).

membrane traffic. The Arf GAPs belonging to ASAP and ACAP subfamily have BAR domains. Homology modeling of the BAR domain of ASAP1 predicts positive electrostatic clusters on the concave surface. We found that, like other BAR domains, the BAR domain of ASAP1 mediates homodimerization and contributes to the formation of tubules from synthetic large unilamellar vesicles in vitro (Nie *et al.*, 2006). Arf contributed to the tubulation induced by ASAP1, supporting the idea that the membrane curvature-inducing function is coupled with Arf signaling.

There are two instances of BAR domains as protein-binding sites. First, arfaptin 2 interacts with Rac small G protein through its BAR domain (Tarricone *et al.*, 2001). The interaction is thought to regulate membrane association of arfaptin. Second, APPL1 is a membrane-trafficking protein that like ASAP1, has a tandem of a BAR and PH domains (Zhu *et al.*, 2007). The two domains fold together to form a binding site for Rab5, which is critical for APPL1 function in endocytosis. These results support the idea that BAR domains function not only as a membrane curvature sensing/inducing domain, but also as a protein-interacting site (Habermann, 2004).

Rab11-family interacting protein 3 (FIP3) is a member of the FIP family of Rab11 binding proteins that may function as Rab11 effectors. FIP3 binds to two different classes of small GTP-binding proteins simultaneously, Rab11 and Arfs (Arf5 and Arf6; Shin *et al.*, 1999; Prekeris, 2003; Fielding *et al.*, 2005). Rab11 is known as a critical regulator for endocytic recycling pathway from recycling endosome to the plasma membrane and for trafficking at the *trans*-Golgi network (TGN) and functions in many cellular events including epithelial polarity, cell adhesion, and cytokinesis that depend on regulated membrane traffic (Zerial and McBride, 2001; van IJzendoorn, 2006). FIP3, like other members of the FIP family, has a Rab11-binding site at its C-terminus (Prekeris, 2003). FIP3 and its closest homolog FIP4 function to maintain the integrity of recycling endosomes and to regulate cytokinesis during interphase and mitotic phase, respectively (Hickson *et al.*, 2003; Wilson *et al.*, 2005; Horgan *et al.*, 2007). Overexpression of FIP3 or FIP4 causes accumulation of recycling endosome at the perinuclear region. This effect is dependent on the ability to bind to Rab11 (Hickson *et al.*, 2003; Horgan *et al.*, 2004). In contrast, depletion of FIP3 induces loss of the perinuclear recycling endosomal compartment (Horgan *et al.*, 2007). Based on these results, FIP3 has been proposed to be a critical regulator of the recycling endosome together with Rab11.

In the experiments reported here, we set out to address two questions about the molecular function of ASAP1. The first question was whether the BAR domain of ASAP1 also serves as a protein-interacting site like the BAR domain of arfaptin. The other question was whether ASAP1 functions in the endocytic pathway. Although ASAP1 is well established as a GAP for Arf proteins, the function of ASAP1 in membrane traffic has remained elusive. Here, we report that ASAP1, through its BAR domain, directly interacts with FIP3. A fraction of ASAP1 colocalizes with FIP3 in the pericentrosomal recycling endosome in HeLa cells and ASAP1 depletion by small interfering RNA (siRNA) disperses TfR-positive endosome from the perinuclear region and perturbs the intracellular trafficking of endocytosed Tfn. Based on these results, we propose that the BAR domain of ASAP1 functions as a protein-interacting site for FIP3 and that ASAP1 participates in Tfn trafficking through the Rab11-dependent pathway.

MATERIALS AND METHODS

Plasmids and Antibodies

ASAP and ACAP constructs are described in Brown *et al.* (1998) and Jackson *et al.* (2000). FIP constructs are described in Prekeris *et al.* (2001) and were kindly provided by Dr. G. W. Gould (University of Glasgow, Glasgow, United Kingdom). cDNA encoding full-length FIP3 was cloned in pEGFP-C3. Deletion mutants of FIP3 were constructed by PCR amplification. Arf and Rab expression plasmids were generous gifts from Drs. J. G. Donaldson, R. Weigert, and Y. Wakabayashi (National Institutes of Health, Bethesda, MD). Site-directed mutagenesis was performed with the QuikChange kit (Stratagene, La Jolla, CA) according to the manufacturer's instructions. Anti-FIP3 polyclonal antibody was produced by immunizing rabbits with purified C-terminal FIP3 (aa 466–756; named FIP3C) fused with glutathione-*S*-transferase (GST; Rockland Immunochemical, Gilbertsville, PA). Then, the antiserum was affinity-purified using a column coupling FIP3C fused with maltose-binding protein. Mouse anti-ASAP1 mAb (clone 19) was from BD Bioscience (Franklin Lakes, NJ). Monoclonal antibodies against FLAG (clone M5), α-tubulin (clone B-5–1-2), γ-tubulin (clone GTU-88), and GST (clone GST-2) were from Sigma (St. Louis, MO). Anti-green fluorescent protein (GFP) polyclonal and monoclonal (clone MMS-118P) antibodies were from Invitrogen (Carlsbad, CA) and Covance (Berkley, CA), respectively. Monoclonal antibodies against Xpress and hemagglutinin (HA; clone MMS-101P) tags were from Invitrogen and Covance, respectively. Anti-His polyclonal antibody was from Santa Cruz Biotechnology (Santa Cruz, CA). Monoclonal antibodies against Arf (Clone 1D9) and GAPDH (clone 6C5) were from Affinity BioReagents (Golden, CO) and BioDesign (Saco, ME), respectively. Anti-Rab11 polyclonal and anti-TfR monoclonal (clone H68.4) antibodies were obtained from Zymed/Invitrogen. Monoclonal antibodies against calnexin (clone 37), GM130 (clone 35), EEA1 (clone 14), and lamp1 (clone H4A3) were from BD Bioscience. Polyclonal antibodies against TGN46 and HA tag were purchased from Abcam (Cambridge, MA).

Cell Culture and Transfections

HeLa, HEK293T, and human glioblastoma U118 cells were maintained in DMEM supplemented with 10% fetal calf serum (FCS), 100 U/ml penicillin, and 100 μg/ml streptomycin at 37°C with 5% CO_2. Cells were plated 1 d before transfection with plasmids using Lipofectamine 2000 (Invitrogen) according to the manufacturer's instructions. Cells were used for assays 24 h after transfection.

Yeast Two-Hybrid Screening

Yeast two-hybrid screening was carried out at Myriad Genetics (Salt Lake City, UT) using the BAR domain of mouse ASAP1 (aa 20–270 and 45–285) as bait with a mating-based method. The corresponding cDNA for ASAP1 BAR domain was cloned into pGBT.superB creating an open reading frame for ASAP1 fragments fused to the GAL4 DNA-binding domain. The bait plasmid was introduced into Myriad's ProNet yeast strain PNY200 (*MATα ura3-52 ade2-101 trp1-901 his3-Δ200 leu2-3112 gal4Δ gal80Δ*). The bait yeast cells were allowed to mate with Myriad's ProNet MATa yeast cells, BK100 (*MAT**a** ura3-52 trp1-901 his3-Δ200 leu2-3112 gal4Δ gal80Δ GAL2-ADE2 LYS2::GAL1-HIS3 met2::GAL7-lacZ*) containing three independent cDNA libraries from human brain, breast/prostate cancer, and mouse embryo. After mating, at least 5 million diploid yeast cells were obtained from each library and selected on His- and Ade-lacking medium. The auxotrophy is suppressed if the bait and prey proteins interact. The prey plasmids were isolated from the positive colonies, and the interaction was confirmed by expression of third reporter gene (lacZ). cDNAs in the positive prey plasmids were sequenced.

RNA Interference

siRNA complexes for human FIP3 were purchased from Dharmacon Research (Boulder, CO) as a pool of four siRNAs (SMARTpool, Cat no. M-021079-00) or from Invitrogen as three individual siRNAs (Stealth select RNAi, Cat no. HSS114589, HSS114590, and HSS114591). The sequences of siRNAs from Invitrogen are 5′-GGACUUCAUCCAGUUUGCUACGGUC-3′, 5′-GCAACUGGACGAGGAGAACAGUGAA-3′, and 5′-GAGAUGAGCUCAUGGAGGCGAUUCA-3′, respectively, based on the human FIP3 sequence. The siRNA pool was used in most experiments. The pool and all of the three individual siRNAs suppressed the protein expression of endogenous FIP3 efficiently (~80% knockdown) and had similar effects on TfR localization (see Figure 7A and Supplemental Figure 2). siRNAs for human ASAP1 were purchased from Invitrogen as three individual siRNAs (Stealth select RNAi, Cat HSS147203, HSS147202 and HSS147204). The sequences of siRNAs are 5′- GACCAGAUCUCUGUCUCGGAGUUCA-3′, 5′- CCCAAAUUGGAGAUUUGCCGCCUAA-3′ and 5′- GGGCAAUAAGGAAUAUGGCAGUGAA-3′, respectively, based on human ASAP1 sequence. In most experiments, they were used as pool of the three. The two individual siRNAs (HSS147202 and HSS147204) suppressed expression of endogenous ASAP1 protein extensively (~80% knockdown) and had the same effect on TfR localization (Figure 7A and Supplemental Figure S2). As a control siRNA, negative control siRNA pool (Dharmacon, Cat no. D-001206-13) was used. All individual or pool siRNAs

were transfected at 30 nM as final concentration in culture medium with Lipofectamine 2000 (Invitrogen). Cells were examined 72 h after transfection.

Coimmunoprecipitation and In Vitro Binding Assay

For immunoprecipitation (IP), HEK293T cells were transfected with the indicated expression vectors in 60-mm dishes. Twenty-four hours after transfection, cells were lysed in IP lysis buffer containing 1% Triton X-100, 150 mM NaCl, 5 mM $MgCl_2$, 100 μM ATP, and 50 mM Tris-HCl, pH 7.4, with protease inhibitor cocktail (Roche Applied Science, Indianapolis, IN). Lysates were cleared by centrifugation. Indicated antibodies and γ-bind beads (GE Healthcare, Little Chalfont, United Kingdom) were added and incubated with the lysates for 2 h at 4°C. After washing five times with IP lysis buffer, precipitated proteins were eluted from the beads by boiling in SDS sample buffer and resolved by SDS-PAGE. The proteins were transferred to PVDF membrane (Bio-Rad, Hercules, CA), and probed with indicated primary antibodies and horseradish peroxidase–labeled secondary antibodies (Jackson ImmunoResearch, West Grove, PA). Proteins were visualized with ECL reagents (GE Healthcare) and Kodak Biomax x-ray films (Carestream Health, Rochester, NY).

For in vitro binding assays, purified recombinant proteins were immobilized on glutathione-, Ni- or γ-bind beads as indicated in each figure. Then counterproteins were incubated with the beads for 3 h at room temperature or overnight at 4°C. After washing three times with binding buffer, bound protein was eluted with SDS sample buffer and detected by immunoblotting using proper antibodies as coimmunoprecipitation or by Coomassie brilliant blue staining.

Arf GAP Assay

Arf GAP assay using ASAP1 was carried out as described previously (Che *et al.*, 2005b; Nie *et al.*, 2006). Briefly, purified myristoylated Arf1 or Arf6 were loaded with [α-^{32}P]GTP in GTP loading buffer (25 mM HEPES, pH 7.4, 100 mM NaCl, 0.5 mM $MgCl_2$, 1 mM EDTA, 1 mM ATP, and 1 mM DTT) with large unilamellar vesicles (LUVs) comprised of 500 μM total phospholipids at 30°C. Purified recombinant ASAP1 BARPZA (aa 1–724) or PZA (aa 325–724) was combined with LUVs (final phospholipids concentration of 500 μM) and purified GST or GST-FIP3C at the indicated concentration in GAP assay cocktail containing 25 mM HEPES, pH 7.4, 100 mM NaCl, 2 mM $MgCl_2$, 1 mM GTP, and 1 mM DTT. ASAP1 BARPZA and PZA were used at final concentrations of 0.3 and 0.7 nM when using Arf1, and of 3.1 and 36 nM when using Arf6 as a substrate that resulted in hydrolysis of ~30% of the GTP bound to Arf. LUVs containing 40% phosphatidylcholine (PC), 25% phosphatidylethanolamine (PE), 15% phosphatidylserine (PS), 10% cholesterol, 9.5% phosphatidylinositol (PI) and 0.5% phosphatidylinositol 4,5-bisphosphate ($PI(4,5)P_2$) were produced by extrusion through a 1-μm pore filter. GAP reactions were initiated by the addition of [α-^{32}P]GTP·Arf to a reaction mixture containing ASAP1 at 30°C. After 3 min the reaction was stopped by dilution with ice-cold stop-buffer (20 mM Tris-HCl, pH 8.0, 100 mM NaCl, 10 mM $MgCl_2$, and 1 mM DTT). Arf protein was trapped on nitrocellulose membrane, and the nucleotides were released from Arf by acid extraction. The nucleotides were separated by polyethylenimino-cellulose thin-layer chromatography and quantified using a Storm PhosphorImager (GE Healthcare). In experiments in which $PI(4,5)P_2$ was titrated, the concentration of PI was adjusted to maintain a total mole fraction of 10% phosphoinositides.

Immunofluorescence and Microscopy

Immunostaining was carried out as previously described (Bharti *et al.*, 2007). For staining of ASAP1, FIP3, TGN46, or α-tubulin, cells were fixed with methanol at −20°C and phosphate-buffered saline (PBS) containing 0.2% bovine serum albumin (BSA), 1% FCS, and 0.04% NaN_3 was used for blocking and antibodies dilution. Confocal microscopy was performed using a Zeiss 510 Meta laser-scanning confocal microscope with a 63×, 1.4 NA Plan-Neofluar oil immersion lens (Carl Zeiss, Thornwood, NY). The Pearson's correlation coefficients were calculated using Imaris software (Bitplane, Zurich, Switzerland). Images for the calculation were captured from three independent experiments with the Zeiss 510 confocal microscope as described above.

Time-Lapse Imaging

Cells were spread on fibronectin-coated chambered cover glass (Nunc, Rochester, NY) overnight and then incubated in serum free DMEM for more than 2 h. Alexa488-Tfn (Invitrogen) was applied to the cells at 150 μg/ml in ice-cold serum-free DMEM and allowed to bind to the cell surface for 1 h on ice. After washing with serum-free medium, the cells were warmed to 37°C on a microscope with prewarmed medium and an environmental chamber (Carl Zeiss) maintained with 5% CO_2 at the time image acquisition was initiated using an inverted Zeiss Axiovert 200 microscope equipped with a Perkin Elmer-Cetus Ultraview spinning disk confocal system (Perkin Elmer, Boston, MA), using a 63× objective oil immersion lens (Carl Zeiss). The images were captured at 2-s intervals for 30 min.

Quantification of the Rate of Tfn Uptake and Recycling

Cells were split into fibronectin-coated 96-well plates and starved with serum-free medium for 2 h. For uptake assays, cells were incubated with biotin-labeled Tfn (Invitrogen; 50 μg/ml as a final concentration) for the indicated time. Uptake was stopped by chilling the cells on ice and washing Tfn from the cell surface with ice-cold acid wash buffer containing 50 mM MES and 150 mM NaCl, pH 5.5. For recycling assays, cells were first saturated with biotin-labeled Tfn for 1 h and washed with the acid wash buffer to remove cell surface Tfn, before incubating the cells for the indicated time. To stop the recycling, cells were chilled on ice and washed with ice-cold acid wash buffer. The cells were fixed with 3.7% formaldehyde in PBS, permeabilized with 0.1% Triton X-100, and blocked with 0.25% BSA, and cell-associated biotin-labeled Tfn was detected with horseradish peroxidase–labeled streptavidin (Pierce, Rockford, IL) and ABTS substrate (Roche). The color development (405 nm) was quantified with Versa Max microplate reader and Soft Max Prosoftware (Molecular Devices, Sunnyvale, CA).

Other Procedures and Reagents

ASAP1 BARPZA, PZA, and BARPH (aa 1–431) protein fragments were purified as described previously (Nie *et al.*, 2006). A fragment comprised of residues 720-1090 of ASAP1 (named YPSH3) was expressed in *Escherichia coli* BL21(DE3) from pET21 as N-terminal T7 tag and C-terminal His tag protein. The protein was purified with Ni-agarose column (Qiagen, Valencia, CA) according to the manufacturer's instruction. Protein concentration was determined using the Bradford assay (Bio-Rad). Other reagents including fibronectin solution were purchased from Sigma-Aldrich if not otherwise specified.

RESULTS

Identification and Characterization of FIP3 as an ASAP1-interacting Protein

To identify a binding protein for BAR domain of ASAP1, two-hybrid screening was carried out using two baits encompassing the BAR domain of ASAP1 (mouse ASAP1 aa 20–270 and aa 45–285) against three independent cDNA libraries from human brain, human breast/prostate cancer, and mouse embryo. At least 5 million of colonies were screened in each library. Twenty-seven candidate proteins were identified (Table 1), including the carboxyl terminal half of FIP3 (FIP3C, residues 466–756) and FIP4 (residues 450–635), which are Rab11- and Arf6-interacting proteins. To focus on function of ASAP1 on membrane trafficking, we further investigated the interaction with the FIP proteins. The interaction of FIP3 with ASAP1 in mammalian cells was examined using IP experiments. First, the BAR domain of ASAP1 fused with FLAG tag or the tagged full-length ASAP1 was expressed with GFP-tagged FIP3C (GFP-FIP3C)

Table 1. Candidates identified by yeast two-hybrid screening with ASAP1 BAR domain

Bait	Identified interactors[a]
Mouse ASAP1 (aa 20–270)	ANAPC7, ASAP2(1006), ASAP2(961), C14ORF166, DNM1(864), GOLGB1, MACF1(5321), MACF1(5938), mARHGEF2, mDTNBP1, MED4, mMACF1(5327), mSESTD1, mUACA, PDE4DIP(1132), **RAB11FIP3(756)**, RAI14, RNF20, SET(290), SH3BP1(750)
Mouse ASAP1 (aa 45–285)	MACF1(5321), mDTNBP1, **mRAB11FIP4**, mRUNDC1, RAI14, RNF20

[a] The numbers in parentheses correspond to isoforms having the amino acid length. Prefixes: m, mouse; no prefix, human. Boldface denotes the carboxyl terminal half of FIP3 (FIP3C, residues 466–756) and FIP4 (residues 450–635), which are Rab11- and Arf6-interacting proteins.

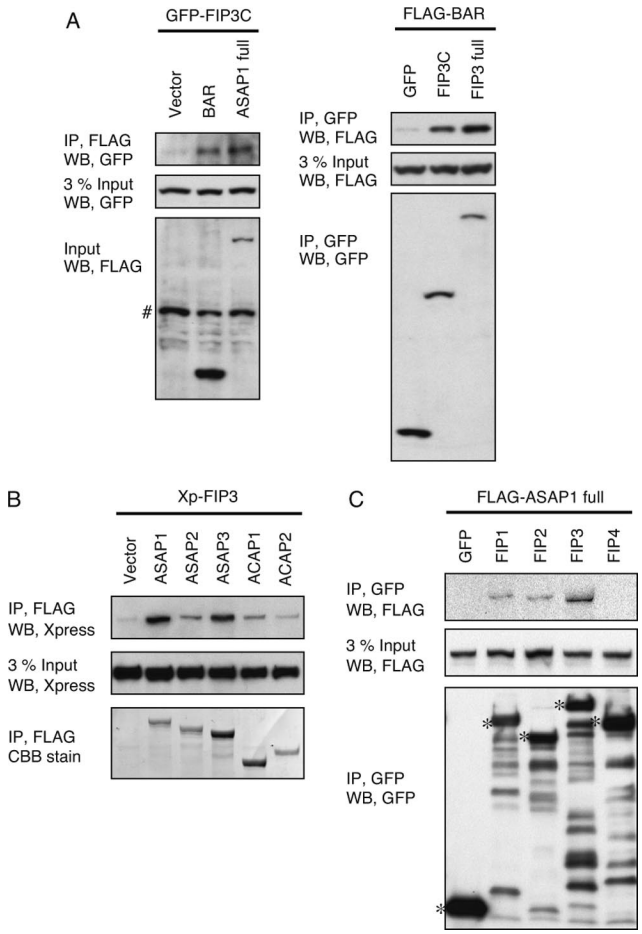

Figure 1. ASAP1 interacts with FIP3. (A) ASAP1 binds to FIP3 in cultured cells. FLAG-tagged full-length protein or BAR domain of ASAP1 was expressed with GFP-tagged full-length protein or C-terminal domain of FIP3 in 293T cells, as indicated, the cells were lysed in IP lysis buffer (see *Materials and Methods*), proteins precipitated by using antibodies indicated at left side of the panels and protein A/G glutathione beads, and precipitated material analyzed by immunoblotting. The protein expression levels in the cell lysates were also determined by immunoblotting. #Nonspecific reactive bands with anti-FLAG antibody. (B) FIP3 interacts with ASAP1 and ASAP3 in BAR domain-containing Arf GAPs. FLAG-tagged Arf GAPs were expressed with Xpress-tagged full-length FIP3 in 293T cells. Immunoprecipitation and immunoblotting were carried out as in A. (C) ASAP1 preferentially interacts with FIP3. GFP-tagged FIP isoforms were expressed with FLAG-tagged ASAP1. Immunoprecipitation and immunoblotting were carried out as in A. *Specific reactive bands for GFP-fused proteins.

in HEK293T cells and precipitated with anti-FLAG antibody. Coprecipitation of GFP-FIP3C was analyzed with immunoblotting using anti-GFP antibody. Both recombinant ASAP1 proteins precipitated FIP3C (Figure 1A, left). The interaction between ASAP1 and FIP3 was also confirmed using GFP-tagged FIP3C or full-length FIP3 with anti-GFP antibody for precipitation (Figure 1A, right). The FLAG-tagged BAR domain of ASAP1 coprecipitated with either full-length FIP3 or FIP3C.

To confirm the interaction between full-length proteins and to determine the isoform specificity for binding to FIP3, BAR domain-containing ArfGAPs including ASAP1, ASAP2, ASAP3, ACAP1, and ACAP2 were tested in similar IP experiments in HEK293T cells (Figure 1B). The strongest signals were observed for ASAP1 and ASAP3, although interaction with other Arf GAPs, including ACAP1, was also detected. Similarly, the binding specificity in FIP isoforms against ASAP1 was analyzed in IP experiments (Figure 1C). ASAP1 preferentially bound to FIP3, although some binding to FIP1 and FIP2 was detected. Conversely, we failed to detect an interaction of ASAP1 to FIP4, although it was isolated by two-hybrid screening using the BAR domain. These results support the idea that ASAP1 forms a complex with FIP3, and we further investigated ASAP1-FIP3 interaction. We cannot exclude the possibility that FIP3 interacts with other Arf GAPs and ASAP1 with other FIP isoforms.

To determine the binding site on each protein, in vitro pulldown assays were carried out using bacterially expressed recombinant proteins derived from ASAP1 and FIP3. Four His-tagged recombinant proteins from ASAP1 were immobilized on γ-bind beads with anti-His polyclonal antibody, and the interaction with GST-FIP3C was analyzed by immunoblotting with anti-GST mAb (Figure 2A). FIP3 interacted with two recombinant proteins containing the BAR domain (BARPZA and BARPH), but not with proteins lacking the BAR domain (PZA and YPSH3). This result supports the idea that the primary binding site of FIP3 on ASAP1 is the BAR domain and that the interaction is direct given that only purified ASAP1 and FIP3 were present.

The ASAP1 binding site on FIP3 was determined by GST-pulldown assay using six deletion mutants of FIP3 (Figure 2Bb, left). Because it is known that FIP3 directly interacts with Rab11 and Arf5/6, their binding sites were also confirmed (Figure 2Bb, right). GST-tagged FIP3 mutants were immobilized on glutathione beads and then incubated with purified ASAP1 BARPZA construct, or HEK293T cell-expressed, GTPγS-loaded Rab11 or Arf5. Rab11 interacted with four C-terminus–containing constructs of FIP3. This indicated that the binding site for Rab11 was at the extreme C-terminus of FIP3 as previously reported (Prekeris *et al.*, 2001). Arf5 bound to two constructs (FIP3C and FIP3C.565) strongly and two constructs (FIP3C.End695 and FIP3C.End651) weakly, consistent with the binding site for Arf5 in the C-terminal half of coiled-coil region of FIP3 as previously reported (Shiba *et al.*, 2006; Schonteich *et al.*, 2007). In contrast, the ASAP1 recombinant protein interacted with four constructs (FIP3C to FIP3C.565) to a similar extent, but much less with two constructs (FIP3C.650 and FIP3C.680) comprised of the C-terminus, supporting the conclusion that ASAP1 binds to the coiled-coil region. This region partially overlaps with the Arf-binding site.

FIP3 binds to Rab11 and Arf6 simultaneously to form a ternary complex (Fielding *et al.*, 2005). We determined whether FIP3 could also form a ternary complex with ASAP1 and Rab11, or Arf (Figure 3). His-tagged ASAP1 BARPZA was immobilized on Ni-agarose beads. After the beads were incubated with or without GST-FIP3C to make ASAP1-FIP3 binary complex, GTPγS-loaded Rab11, Arf1·GTPγS, Arf5·GTPγS or Arf6·GTPγS was overlaid on the beads for 3 h at room temperature. The beads were washed and Rab11 and Arf that associated with the beads were analyzed by immunoblotting. Rab11 was efficiently precipitated when FIP3C was added to the beads. In contrast, adding FIP3C did not result in the precipitation of either Arf5 or Arf6 (Figure 3). The signals observed were the same as that seen with Ni-beads alone. In this experiment, Arf1 was included under one condition was used as a negative control. These results support the conclusion that ASAP1 can bind to Rab11 through FIP3 to form a ternary complex.

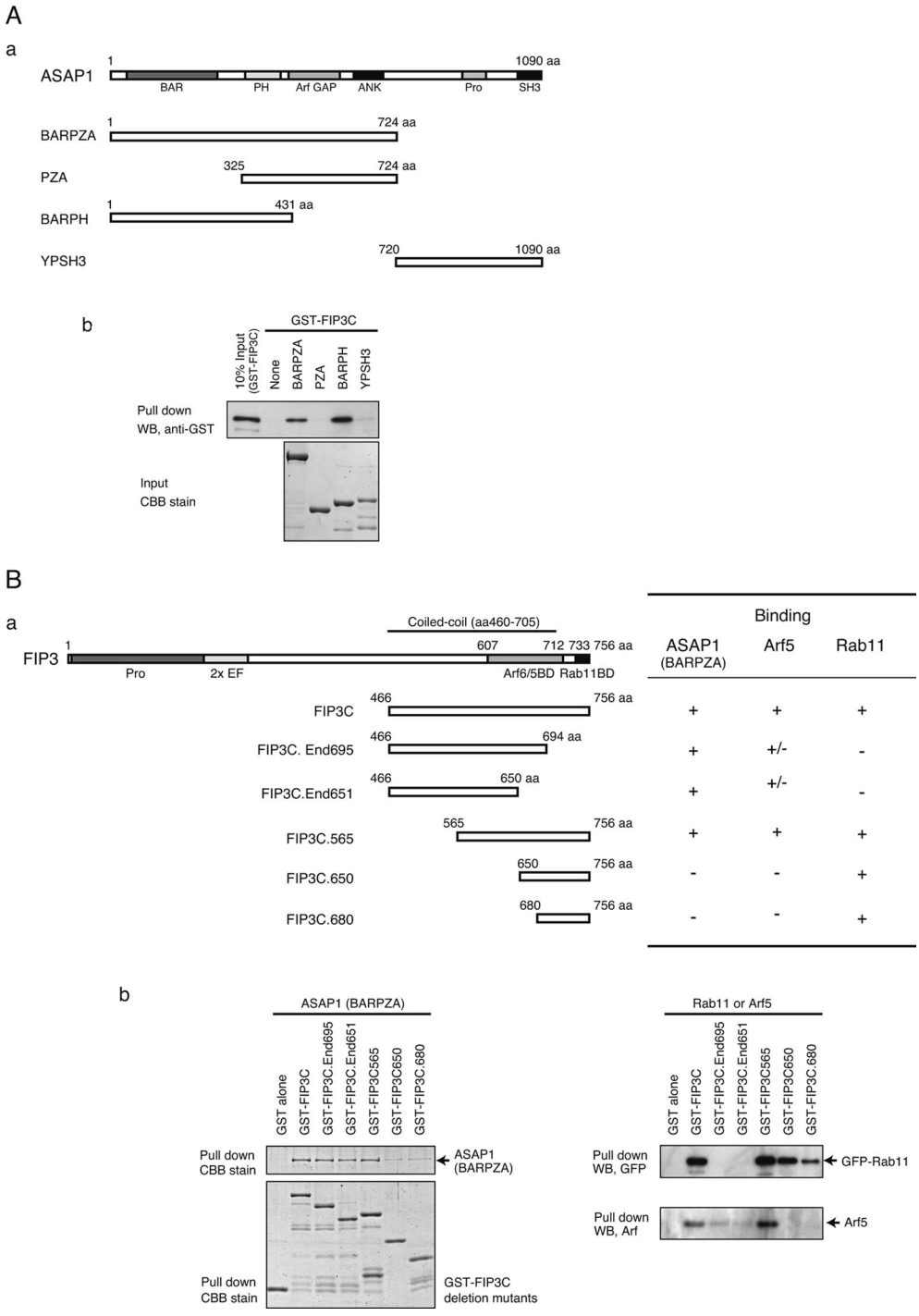

Figure 2. ASAP1 BAR domain associates with the C-terminal coiled-coil region of FIP3. (A) FIP3 directly binds to ASAP1 BAR domain. (a) Schematic representation of ASAP1 domain structure and its deletion mutants. Abbreviation of domains is as follows: BAR, BAR (Bin-Amphiphysin-Rvs); PH, pleckstrin homology; Arf GAP, Arf GAP; ANK, Ankyrin repeat; Pro, proline rich region; and SH3, Src homology 3. (b) Pulldown assay of ASAP1 deletion mutants with FIP3. Bacterially expressed, purified ASAP1 deletion proteins were immobilized on γ-bind beads with polyclonal antibody against the His tag and incubated with purified GST-FIP3C (aa.466–756) at the concentration of 0.3 μM of ASAP1 proteins and 0.15 μM GST-FIP3C in 1× GAP buffer (0.1% Triton X-100, 25 mM HEPES, pH 7.4, 100 mM NaCl, 2 mM $MgCl_2$, 1 mM GTP sodium salt, and 1 mM DTT) for 3 h at room temperature. After washing, the protein complexes precipitated with the beads were analyzed by immunoblotting. (B) ASAP1 binds to the middle of the C-terminal coiled-coil region of FIP3, which is N-terminal of Arf5- and Rab11-binding sites. (a) Schematic representation of FIP3 domain structure and its deletion mutants and a summary of the pulldown assay. Abbreviations for the domains are as follows: Pro, Proline rich region; 2× EF, a tandem repeat of EF hands; Arf6/5BD, Arf6- or 5-binding domain; Rab11BD, Rab11-binding domain. (b) Pulldown assay of FIP3 deletion mutants with ASAP1, Rab11, or Arf5. Bacterially expressed, purified ASAP1 BARPZA proteins, or 293T cell–expressed, GTPγS-loaded Rab11 or Arf5 was incubated with GST-fused FIP3 deletion mutants immobilized on glutathione beads as in A except for the addition of 10 μM GTPγS in the experiments for Rab11 and Arf5. After extensive washing, the interactions were detected on SDS-PAGE followed by CBB staining or immunoblotting using the indicated antibodies.

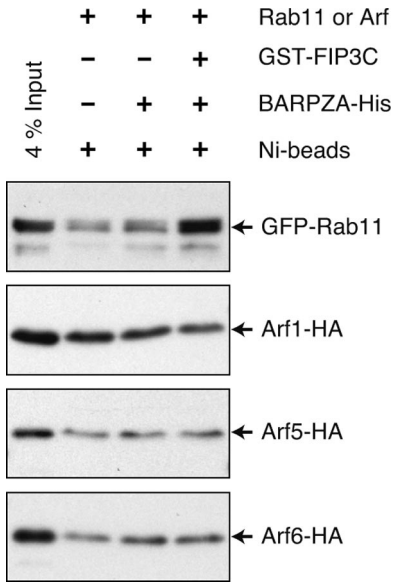

Figure 3. ASAP1 is able to form ternary complex with Rab11 through FIP3. ASAP1 BARPZA alone or the BARPZA and GST-FIP3C complexes were immobilized on Ni-beads and then incubated with GTPγS-loaded GFP-Rab11, Arf1-HA, Arf5-HA, or Arf6-HA (expressed in 293T cells) in a buffer containing 0.5% Triton X-100, 20 mM Tris-HCl, pH 8.0, 300 mM NaCl, 10 mM imidazole, 0.5 mM $MgCl_2$, 1 mM EDTA, and 1 mM 2-mercaptoethanol for 3 h at room temperature. After extensive washing, precipitated materials were eluted with SDS-containing buffer and analyzed by immunoblotting using anti-GFP or anti-HA antibodies.

FIP3 Activates ASAP1 Arf GAP Activity

ASAP1 is an Arf GTPase-activating protein that prefers Arf1 and Arf5 to Arf6 (Brown *et al.*, 1998; Furman *et al.*, 2002; Liu *et al.*, 2005). Because FIP3 directly binds to the BAR domain of ASAP1 as described above, we investigated whether the interaction regulates the Arf GAP activity of ASAP1 (Figure 4A). Recombinant ASAP1 proteins, BARPZA or PZA, were incubated with purified GST-FIP3C or GST alone at the indicated concentration for 30 min in GAP reaction buffer, and then the reactions were started by adding [α-^{32}P]GTP-loaded Arf. LUVs, 500 μM, containing 0.5% $PI(4,5)P_2$ was included in the reactions. GST-FIP3C stimulated GAP activity of ASAP1 BARPZA against Arf1 by 2.5-fold (Figure 4A, left). The concentration of FIP3 that gave 50% of the maximal effect was about 0.3 μM. This effect was not observed when ASAP1 PZA, which lacks the BAR domain, was used instead of BARPZA. GST had no effect on the GAP activities of either ASAP1 BARPZA or PZA. In contrast to Arf1, when Arf6 was used as substrate, FIP3C did not stimulate GAP activity (Figure 4A, right).

ASAP1 has a PH domain next to the BAR domain, which binds preferentially to $PI(4,5)P_2$, which stimulates GAP activity (Kam *et al.*, 2000; Che *et al.*, 2005a). Because FIP3 also stimulates the activity, we tested whether $PI(4,5)P_2$ and FIP3 are synergistic. We carried out the GAP assay for ASAP1 BARPZA and myristoylated Arf1 with the same method as Figure 4A except using LUVs containing $PI(4,5)P_2$ at the indicated concentrations. GST-FIP3C or GST was added at 1500 nM. Without FIP3 (GST alone), the concentration dependence of $PI(4,5)P_2$ stimulation of GAP activity was hyperbolic as previously reported (Figure 4B; Kam *et al.*, 2000). In the presence of GST-FIP3C, the effect of $PI(4,5)P_2$ was biphasic with a maximum stimulation seen with 0.5% $PI(4,5)P_2$ in 500 μM LUVs. The effect of 0.5% $PI(4,5)P_2$ and 1500 nM FIP3 together was greater than either $PI(4,5)P_2$ or FIP3 alone.

To further define the interaction of $PI(4,5)P_2$ and FIP3 with ASAP1, we examined the effect of $PI(4,5)P_2$ on FIP3 binding to ASAP1 (Figure 5). We determined the effect of $PI(4,5)P_2$ on the amount of ASAP1 BARPZA that coprecipitated with GST-FIP3C. For this experiment, we used 45 μM $PI(4,5)P_2$ in mixed Triton X-100 micelles. This concentration of $PI(4,5)P_2$ corresponds to ~10% in 500 μM LUVs. In the absence of $PI(4,5)P_2$, the amount of ASAP1 in the precipitate was dependent on the concentration of GST-FIP3C, with more than 100 ng of ASAP1 bound to 1.5 μM FIP3C (Figure 5B). Precipitation of ASAP1 was reduced by 80% by the addition of $PI(4,5)P_2$. These results suggest that although FIP3 stimulates ASAP1 GAP activity against Arf1 synergistically with $PI(4,5)P_2$, high concentration of $PI(4,5)P_2$ prevent ASAP1-FIP3 interaction.

ASAP1 Colocalizes with FIP3 in the Pericentrosomal Endocytic Recycling Compartment

FIP3 localizes with pericentrosomal recycling endosomes and the midbody during interphase and mitotic phase, respectively, in HeLa cells (Horgan *et al.*, 2004; Wilson *et al.*, 2005). FIP4, which is the closest isoform of FIP3 in the FIP family, is also found in pericentrosomal recycling endosomes and the midbody, and small fraction is in centrosomes and focal adhesion (Hickson *et al.*, 2003). Moreover, Nuf, the *Drosophila* orthologue of mammalian FIP3 and FIP4, associates with the pericentrosomal recycling endosomes during cellularization, and a *nuf* mutant disrupts recruitment of actin to the cortical cleavage furrow (Riggs *et al.*, 2003). ASAP1 is cytoplasmic and in cell adhesion sites including focal adhesions, invadopodia, and podosomes in fibroblasts and invasive epithelial tumor cells (Randazzo *et al.*, 2000; Onodera *et al.*, 2005; Bharti *et al.*, 2007). The interaction of ASAP1 with FIP3 described above led us to consider the possibility that the two proteins operate together in the endocytic recycling compartment or cell adhesion sites. To define the functional site of the ASAP1-FIP3 complex in cells, the endogenous proteins were stained using specific antibodies in HeLa cells and human glioblastoma U118 cells. ASAP1 and FIP3 colocalized in perinuclear dot-like structures (Figure 6A, top). FIP3 localization varied from the single dot to more broad vesicular structures at the perinuclear region (Figure 6A, bottom). To determine the localization of ASAP1, a number of antibodies were tested for visualizing ASAP1 in fixed cells. All were specific ASAP1 but identified different subpopulations of the protein. The antibody used for the experiments presented in Figure 6 was characterized as described in Supplemental Figure S1. It identified a population of ASAP1 in well-demarcated perinuclear dots (Figure 6, A and C). The ASAP1-positive dots colocalized with the most prominent FIP3-positive vesicles even in cells showing a more diffuse staining pattern for FIP3 (Figure 6A, bottom). The Pearson's r for ASAP1-FIP3 localization was 0.55 (SEM, 0.05; n = 12); In the two patterns of cells with FIP3 dot-like or broad vesicular structures, they were 0.59 and 0.47, suggesting ASAP1 and FIP3 were significantly colocalized in both cases. The antibody signals in the perinuclear dots were significantly diminished by preincubating the antibodies with antigens and were not detectable with nonimmune IgG (Supplemental Figure S1 and see *Discussion*). To determine if these FIP3- and ASAP1-positive structures are pericentrosomal recycling endosomes as previously reported (Hickson *et al.*, 2003; Horgan *et al.*, 2004), cells were stained for either TfR or Rab11, markers of

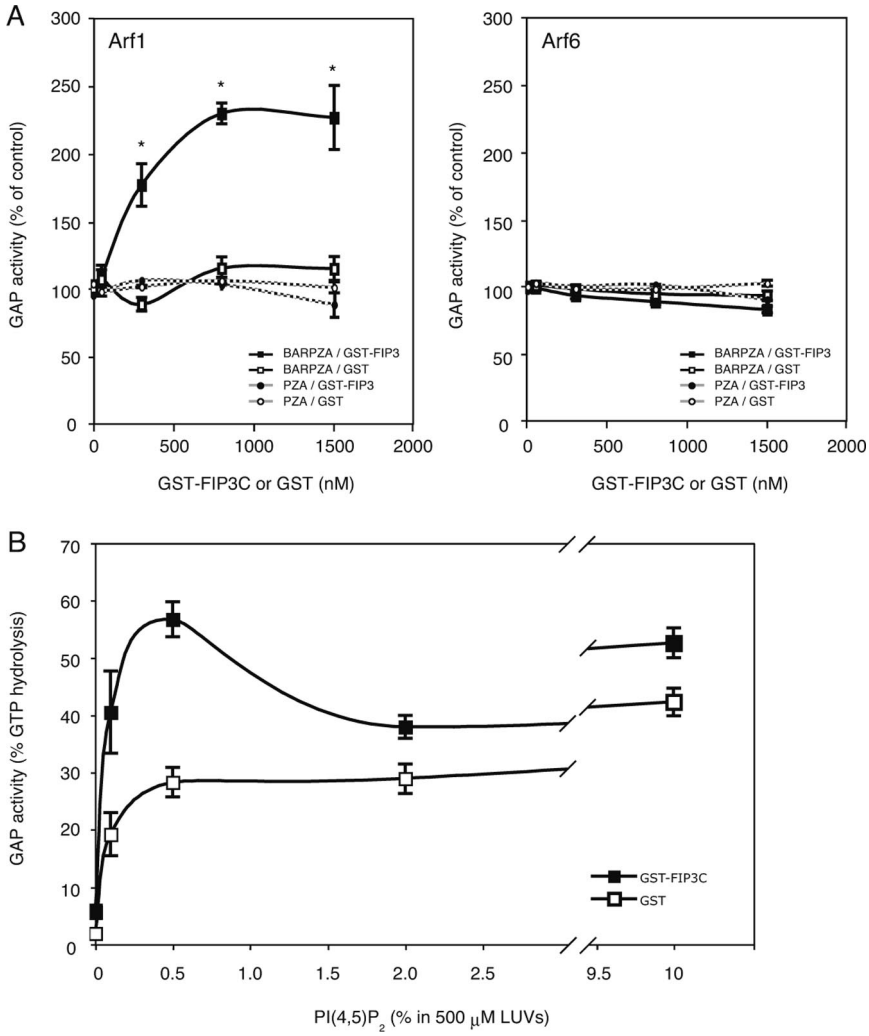

Figure 4. FIP3 stimulates ASAP1 GAP activity against Arf1. (A) FIP3 stimulates ASAP1 GAP activity against Arf1, but not Arf6. Purified ASAP1 proteins with or without BAR domain, BARPZA or PZA, were preincubated with GST-FIP3C or GST alone for 30 min at room temperature before addition of [α-^{32}P]GTP-loaded myristoylated Arf1 (left) or myristoylated Arf6 (right). LUVs prepared as described in *Materials and Methods* were included in the assays. The reaction was stopped after 3 min, and the amount of GTP hydrolyzed was quantified as described in *Materials and Methods.* The data are from three independent experiments performed in duplicate. Error bars, SEM; *$p < 0.01$ compared with the value in 0 nM GST-FIP3C as analyzed by ANOVA followed by a Dunnett test. ■, BARPZA with GST-FIP3C; □, BARPZA with GST; ●, PZA with GST-FIP3C; ○, PZA with GST. (B) PI(4,5)P_2 effect on Arf GAP activity is biphasic in the presence of FIP3. Purified ASAP1 BARPZA was preincubated with 1500 nM GST-FIP3 for 30 min at room temperature. Myristoylated Arf1 was loaded with [α-^{32}P]GTP using LUVs containing the indicated concentration of PI(4,5)P_2. The GAP reactions were initiated by the addition of GTP·Arf1 into the reaction mixture including ASAP1 BARPZA, GST-FIP3, and LUVs with the indicated concentration of PI(4,5)P_2. Termination of the reactions and data collection are described in A. The data are from seven independent experiments performed in duplicate. Error bars, SEM.

recycling endosomes. FIP3 and ASAP1 colocalized with these markers in the perinuclear region (Figure 6, B and C). The Pearson's r for TfR-FIP3 and Rab11-ASAP1 were 0.56 (SEM, 0.02; n = 11) and 0.48 (SEM, 0.03; n = 9), respectively. These results support the conclusion that ASAP1 and FIP3 associate with the endocytic recycling compartment.

ASAP1 and FIP3 Are Required for Perinuclear Localization of Transferrin and Its Receptor

FIP3 is involved in the accumulation of recycling endosome in the pericentrosomal region (Horgan *et al.*, 2007). To define the function of ASAP1 in the endocytic recycling compartment, endogenous ASAP1 or FIP3 was depleted using siRNAs in HeLa cells. Expression levels were examined by immunoblot analysis (Figure 7A and Supplemental Figure S2). Both ASAP1 and FIP3 were efficiently depleted. Using these cells, immunostaining experiments against TfR were carried out (Figure 7B). In the cells transfected with control siRNA, TfR accumulated in the perinuclear region as in nontransfected cells (compare Figure 7B with 6B). In contrast, in ASAP1-depleted cells, TfR accumulated at the cell edge to a greater extent than the perinuclear region (Figure 7, B and C). In FIP3-depleted cells, the distribution of TfR was changed from the perinuclear region to a diffuse pattern over the whole cell body (Figure 7, B and C). It is noteworthy that FIP3 depletion was more potent than ASAP1 depletion for attenuation of perinuclear accumulation of TfR. These results support the idea that ASAP1, like FIP3, is essential for the pericentrosomal localization of recycling endosomes containing TfR.

To evaluate whether the effects of ASAP1 or FIP3 depletion are specific to recycling endosome, we checked the localization of other organelles in ASAP1- or FIP3-depleted cells (Supplemental Figure S3). Cells were stained for the endoplasmic reticulum (ER) marker calnexin, the Golgi apparatus marker GM130, TGN marker TGN46, early endosome marker EEA1, late endosome and lysosome marker lamp1, and cytoskeleton microtubules. The localization of these organelle markers was not affected by ASAP1 or FIP3 depletion. These results are consistent with specific effects of ASAP1 and FIP3 function on recycling endosomes.

Pulse-chase experiments with fluorescence-labeled Tfn were carried out to determine whether ASAP1 or FIP3 depletion affected trafficking of endocytosed Tfn (Figure 8A). Ten minutes after chase, in either cells transfected with control, ASAP1, or FIP3 siRNA, endocytosed Tfn was observed as small dot structures over most of the cell body with some accumulation at the cell edge in ASAP1-depleted cells. Thirty minutes after chase was initiated, Tfn accumulated in the perinuclear region in cells treated with control

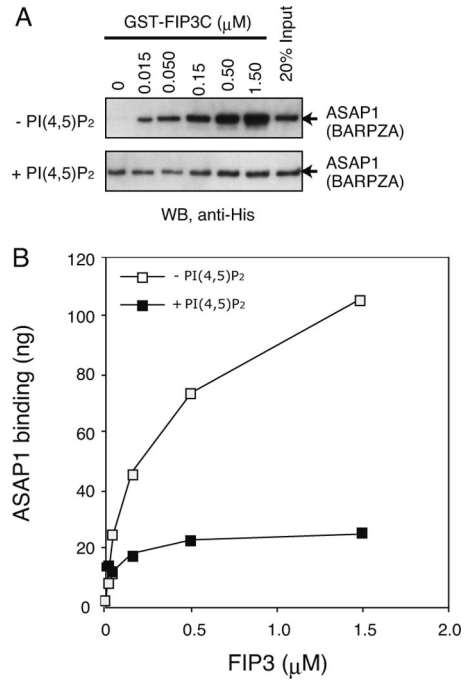

Figure 5. ASAP1-FIP3 interaction is inhibited by PI(4,5)P_2. (A) Representative result showing inhibitory effect of PI(4,5)P_2 on ASAP1-FIP3 interaction. GST-FIP3C was immobilized on glutathione beads and incubated with His-tagged ASAP1 BARPZA for 3 h at room temperature in the buffer indicated in Figure 2A with or without 45 μM PI(4,5)P_2. The lipid was presented as a mixed micelle with 0.1% Triton X-100 micelle. After washing, precipitated ASAP1 BARPZA was detected by immunoblotting using anti-His antibody. (B) Quantitation of data from A. The amount of precipitated ASAP1 with GST-FIP3C beads was quantified by comparison of the ECL signals to those of standards of purified ASAP1 BARPZA included in the same immunoblot.

siRNA. In contrast, in ASAP1-depleted cells, Tfn remained in the cell periphery. In FIP3-depleted cells, Tfn remained in puncta diffusely dispersed through the cell. After 60 min, most of Tfn was recycled out of the cells transfected with either siRNA. Despite the differences in cellular localization, the rate of Tfn uptake (Figure 8B) and recycling (Figure 8C) were similar in the control, ASAP1-, or FIP3-depleted cells.

Live cell imaging of endocytosed fluorescence-labeled Tfn was also examined. In control siRNA-transfected cells, endocytosed Tfn was first visualized as small puncta, presumably enodocytic vesicles, throughout the cell and then accumulated in the perinuclear region. The Tfn in the perinuclear region moved in and out as tubulovesicular structures (Figure 8D and Supplemental Movie 1). In ASAP1-depleted cells, the endocytosed Tfn was first observed as small vesicular structures dispersed throughout the cell as in the control cells. Over time, most Tfn accumulated at the cell edge, although a small fraction associated with perinuclear structures (Figure 8D and Supplemental Movie 2). In FIP3-depleted cells, the vesicles containing Tfn moved randomly in the cell without accumulation at a particular region or site, similar to the distribution observed in fixed cells (Figure 8D and Supplemental Movie 3). Tubulovesicular structures were not observed in either ASAP1- or FIP3-depleted cells. These results are consistent with the conclusion that ASAP1 and FIP3 function as regulators of the pericentrosomal localization of Tfn and its receptor.

We further characterized the peripheral TfR-positive endosomes induced by ASAP1 depletion. There was a possibility that the peripheral TfR-positive vesicles were an early endosome or endosomal intermediate. To address this question, GFP-tagged Rab5, an early endosome marker, or Rab11 were expressed in ASAP1-depleted HeLa cells. To minimize the effect of overexpressing these GTP-binding proteins, the cells having the lowest level of the expression were examined (Figure 9A). We found the peripheral TfR-positive vesicles were relatively close to GFP-Rab5-positive puncta, but their colocalization was very limited. In contrast, GFP-Rab11 colocalized with the ASAP1-induced peripheral vesicles.

We also determined whether these vesicles contain Arf1 or Arf6 reasoning that depletion of ASAP1 may change the subcellular distribution of its potential substrates (Figure 9B). Arf1 and Arf6, both c-terminally tagged with HA, were expressed in cells transfected with control or ASAP1 siRNA. In control siRNA-transfected cells, the distribution of the Arfs was similar to that previously reported, with Arf1 associated with Golgi-like structures and Arf6 with the plasma membrane and tubulovesicular structures (D'Souza-Schorey and Chavrier, 2006). A small amount of Arf1 and Arf6 was detected on TfR-positive vesicles at the perinuclear region. As described above, ASAP1 depletion altered the distribution of TfR-positive vesicles. In the ASAP1-depleted cells, the fraction of Arf1-HA that resides on TfR-positive endosome significantly decreased, but a small amount of Arf1-HA associated with the cell edge and, as observed in the controls, in some of the TfR-positive vesicles. Arf6-HA also associated with vesicular structures and some tubular structures containing TfR (Figure 9B).

Finally, we examined the effect of ASAP1 or FIP3 depletion on the localization of the other. In ASAP1-depleted cells, a large fraction of FIP3 relocated from the perinuclear region to cell edge as associating with TfR (Figure 10A, compare to Figure 6B). In FIP3-depleted cells, ASAP1 was still at the perinuclear region. Rab11 was dispersed throughout the cell as previously reported (Horgan *et al.*, 2007), but some Rab11 was present with ASAP1(Figure 10B, inset 1). Rab11 on the vesicles throughout the cell rarely colocalized with ASAP1 (Figure 10B, inset 2). These data support the idea that ASAP1 and FIP3 are independent each other for the organelle association of them.

DISCUSSION

In this study, we examined the hypothesis that the BAR domain of ASAP1 is a protein binding site. Consistent with the hypothesis, we identified the Rab11-interacting protein FIP3 as a binding partner. The interaction of the BAR domain is with the coiled-coil domain of FIP3 and leads to a ternary complex of ASAP1, FIP3, and Rab11. Like FIP3, ASAP1 regulates positioning of the recycling endosome that contains transferrin receptor. To our knowledge, this is the first report that the BAR domain of ASAP1 functions as a protein-binding site and the first report of this mode of protein interaction with a BAR domain.

The BAR domain superfamily is comprised of BAR/N-BAR, F-BAR, and I-BAR. The members of the family are distinguished from each other in their secondary and tertiary structures and the extent of curvature of membrane that they are associated with (Fütterer and Machesky, 2007). Canonical BAR domains including ASAP1 BAR consist of three long, kinked α-helices that are bundled to form crescent-shaped homodimers (Peter *et al.*, 2004). Several BAR domains found in amphipysin, endophilin, sorting nexins and Arf GAPs such as ACAP1 and ASAP1 sense or induce

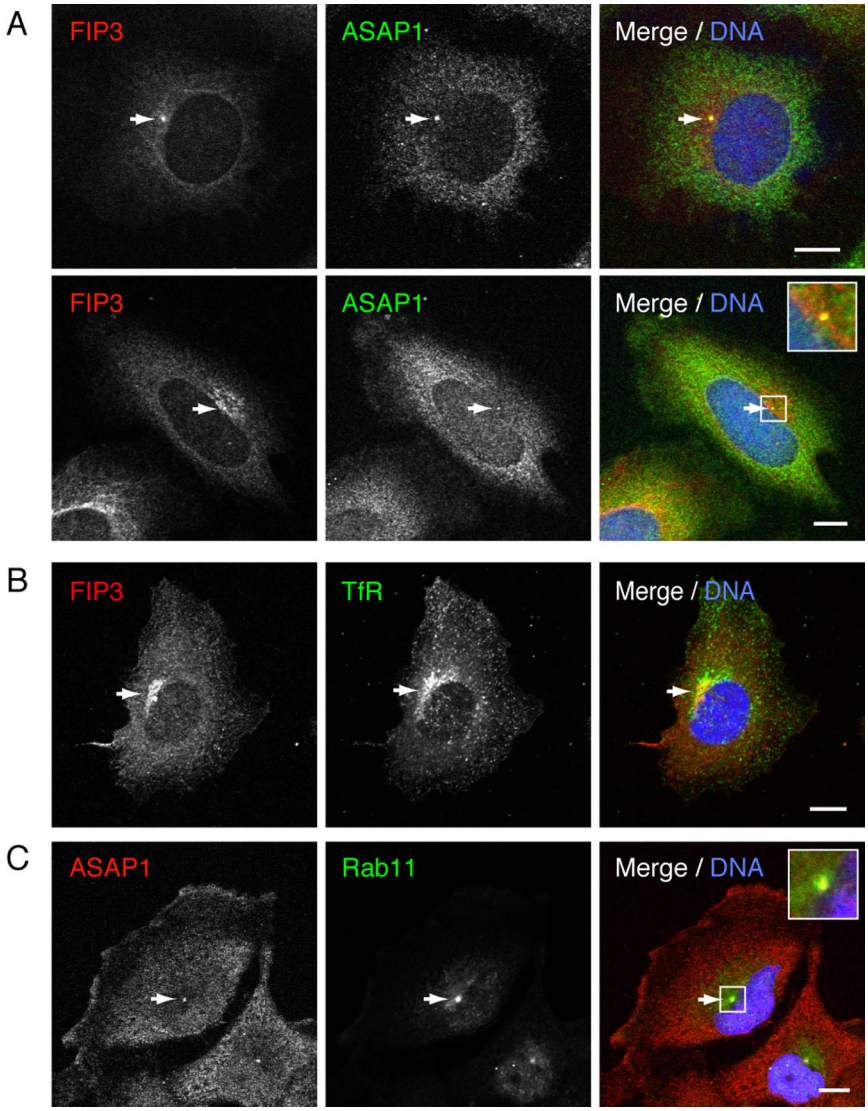

Figure 6. ASAP1 associates with the FIP3-positive pericentrosomal endocytic recycling compartment in HeLa cells and U118 cells. HeLa cells (A and B) or U118 cells (C) were seeded on fibronectin-coated cover glass, cultured in DMEM containing 10% FCS overnight, fixed with cold methanol, and then stained with antibodies against the indicated proteins. Images were captured with a Zeiss 510 Meta laser-scanning confocal microscope with a 63×, 1.4 NA Plan-Neofluar oil immersion lens. Arrows indicate the area where the two proteins are colocalized. Boxed areas are enlarged as insets. Bar, 10 μm.

membrane curvature (Takei *et al.*, 1999; Carlton *et al.*, 2004; Peter *et al.*, 2004; Masuda *et al.*, 2006; Nie *et al.*, 2006). Other BAR proteins, arfaptin 2 and APPL1, interact with small G proteins (Tarricone *et al.*, 2001; Miaczynska *et al.*, 2004). In our study, we found that the BAR domain of ASAP1 directly interacts with the coiled-coil domain of FIP3. This is a first report, to our knowledge, of a BAR domain interacting with a protein other than small G proteins. The interaction is through the coiled-coil region of both proteins and, therefore, represents another mode of interaction with BAR domains. A Pfam functional domain search identified similarities of both the ASAP1 BAR and FIP3 coiled-coil domains with IMP dehydrogenase (IMPDH)/GMP reductase domain. IMPDH forms a homotetramer through its core domain (Sintchak *et al.*, 1996). Because both ASAP1 and FIP3 form homodimers (Eathiraj *et al.*, 2006; Nie *et al.*, 2006; Shiba *et al.*, 2006), they might function as heterotetramer.

FIP3 is comprised of an N-terminal Pro-rich domain, two EF-hand motifs and, in the C-terminal half of the molecule, a coiled-coil domain. Rab11 and Arf5/6 bind to C-terminal end and C-terminal half of the coiled-coil domain, respectively (Prekeris *et al.*, 2001; Shiba *et al.*, 2006; Schonteich *et al.*, 2007). The domain also mediates homodimerization and heterodimer formation with other FIPs, which also contain coiled-coil domain in their C-terminal region (Wallace *et al.*, 2002; Eathiraj *et al.*, 2006; Shiba *et al.*, 2006; Horgan *et al.*, 2007). We found the ASAP1 BAR domain binds to the middle of the FIP3 coiled-coil domain. The interaction may regulate FIP3-Arfs interaction or FIP3 homo- or heterodimer formation with other FIPs, because the interacting sites at least partly overlap.

The GAP activity of ASAP1 is stimulated specifically by the signaling lipid PI(4,5)P_2 (Brown *et al.*, 1998). PI(4,5)P_2 binds to the PH domain of ASAP1, which can serve to both recruit ASAP1 to a membrane surface and to induce an activating conformational change in the protein (Kam *et al.*, 2000; Che *et al.*, 2005a). In this study, we found FIP3 stimulates ASAP1 GAP activity toward Arf1. This effect of FIP3 on ASAP1 was dependent on the BAR domain of ASAP1. The activation by FIP3 was observed only when myristoylated Arf1 was used as a substrate with LUVs as a lipid source. We did not observe the effect if nonmyristoylated Arf was used as a substrate or if Triton micelles were used in place of LUVs (data not shown). These observations suggest the activation is dependent on association with a phospholipids bilayer and might be coupled with a change in a physical

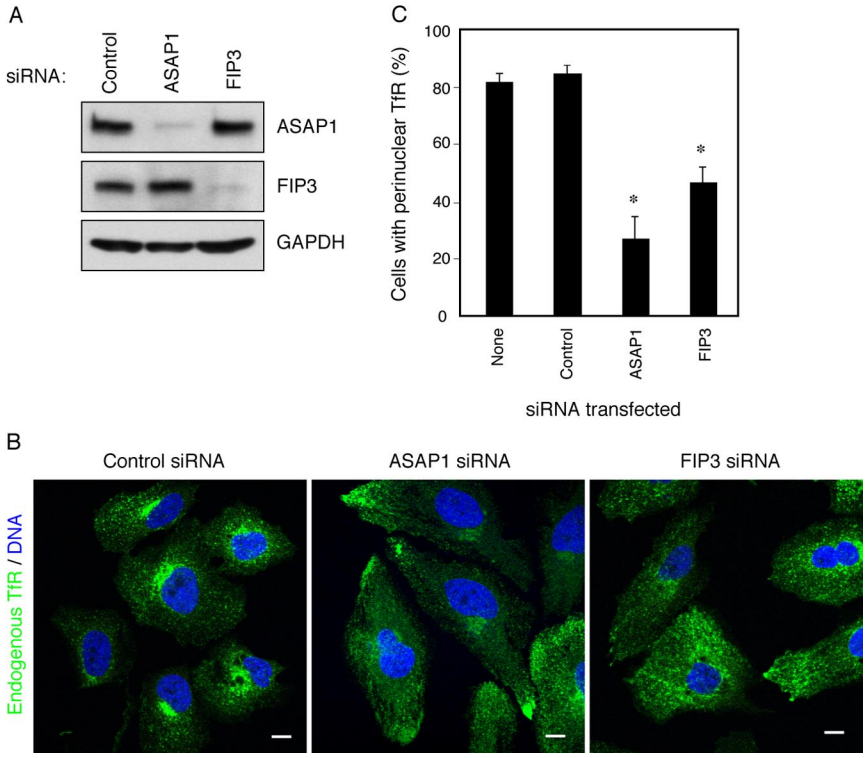

Figure 7. Depletion of ASAP1 or FIP3 affects subcellular distribution of TfR. (A) Depletion of ASAP1 or FIP3 by siRNA. HeLa cells were transfected with siRNA for nontargeting control, ASAP1, or FIP3. Seventy-two hours after transfection, the cells were lysed in RIPA buffer containing 1% IGEPAL-CA630, 0.5% Na deoxycholate, 0.1% SDS, 150 mM NaCl, 20 mM Tris-HCl, pH 7.5, and Protease inhibitor cocktail (Roche). The lysates were subjected to SDS-PAGE, and the indicated proteins were detected with specific antibodies. Glyceraldehyde 3-phosphate dehydrogenase (GAPDH) was used as a loading control. (B) Depletion of ASAP1 causes peripheral accumulation of TfR. ASAP1- or FIP3-depleted HeLa cells were fixed with formaldehyde and then stained with anti-TfR antibody and Hoechst 33342. Images were taken as shown in Figure 6. Bar, 10 μm. (C) Quantitation of the effect of ASAP1 or FIP3 depletion. Cells from the experiment described in B were scored for the presence of the most significant accumulation of TfR at the perinuclear region in the cell. At least 100 cells were counted for each experiment. The values presented are means ± SDs of three independent experiments. *$p < 0.01$ compared with the value in nontransfected cells (None) as analyzed by ANOVA followed by a Dunnett test.

property of the membrane, such as tubulation. The activation of GAP activity by FIP3 supports the idea that FIP3 directly interacts with ASAP1.

The role of FIP3 in stimulating GAP activity is complex. In the presence of FIP3, the effect of $PI(4,5)P_2$ on GAP activity was biphasic. The molecular basis for the biphasic response can be explained, in part, by inhibition of ASAP1-FIP3 interaction by a higher concentration of $PI(4,5)P_2$. Although further investigation is required to fully understand the interplay between FIP3 and $PI(4,5)P_2$ on the physiological regulation of ASAP1, a plausible hypothesis is that FIP3 and $PI(4,5)P_2$ function at different cellular sites. For example, $PI(4,5)P_2$ is enriched at the plasma membrane where it may stimulate ASAP1 (Haucke, 2005). FIP3 might stimulate GAP activity on the recycling endosome membrane. $PI(4,5)P_2$ might inhibit the interaction of ASAP1 and FIP3 on the plasma membrane to block other functions of FIP3 at this site. Another possibility is that the relationship of FIP3 and $PI(4,5)P_2$ binding gives temporal direction to biochemical events regulated by ASAP1. For instance, Arf1·GTP, produced by a regulated exchange factor, could bind to PI 4-P 5-kinase, activating the enzyme, which results in the production of $PI(4,5)P_2$. $PI(4,5)P_2$ would help target ASAP1 to the membrane where it would also interact with other membrane components, such as proteins. On the membrane, ASAP1 would convert Arf1·GTP to Arf1·GDP, with a consequent decrease of $PI(4,5)P_2$ production. Subsequently, ASAP1 could bind FIP3.

The physiological substrate for ASAP1 GAP activity remains an open question. FIP3 preferentially binds to Arf6 and Arf5 (Shin *et al.*, 2001; Hickson *et al.*, 2003; Fielding *et al.*, 2005). We found FIP3 interaction stimulates ASAP1 GAP activity against Arf1, but not against Arf6. In addition to its function at the Golgi apparatus, Arf1 is thought to have similar functions at other cellular locations such as TGN, endosome, and the plasma membrane (Shin *et al.*, 2004; Pagano *et al.*, 2004; D'Souza-Schorey and Chavrier, 2006; Cohen *et al.*, 2007; Kumari and Mayor, 2008). A recent report has suggested a model in which Arf6 indirectly recruits activated Arf1 to the plasma membrane (Cohen *et al.*, 2007). ARNO, a guanine nucleotide exchange factor for Arf1, binds to the plasma membrane by directly interacting with Arf6 through its PH domain and activates Arf1 at the membrane. This mechanism involves cooperation between Arf isoforms. Because FIP3 interacts with Arf6 and ASAP1 uses Arf1 as a substrate, the FIP3-ASAP1 complex may functionally couple Arf6 with Arf1 at the membrane of a recycling endosome. Although FIP3 enhances ASAP1 GAP activity against Arf1, our data do not exclude other Arf isoforms as substrates. Indeed, Arf3 has high homology to Arf1 (~95% identity on the primary amino acid sequences), and our previous in vitro analysis has shown that Arf5 is as efficiently used by ASAP1 as Arf1 (Brown *et al.*, 1998). Furthermore, we cannot exclude the possibility that ASAP1 regulates Arf6 catalysis within the FIP3 complex, because it has been proposed that ASAP2/AMAP2, the closest isoform of ASAP1, sustains the active state of Arf6 through a direct interaction and slow catalysis (Hashimoto *et al.*, 2004). Our results also raise the possibility that ASAP1 indirectly binds to Arf6 through FIP3.

In this report, we found that ASAP1 functions in the pericentrosomal recycling endosomal compartment in HeLa cells. ASAP1 has previously been reported to function in peripheral cellular sites including focal adhesions, invadopodia/podosome and circular dorsal ruffles where the actin cytoskeleton is remodeled (Randazzo *et al.*, 2000; Onodera *et al.*, 2005; Bharti *et al.*, 2007). Function of ASAP1 at recycling endosomes may be related to that in the cell periphery. In cell migration, invasion, and scattering of epithelial cells, both Arf6 and Rab11 are involved in the trafficking of adhesion molecules including integrins and cadherin between recycling endosome and the plasma membrane (Brown *et al.*, 2001; Santy and Casanova, 2001; Powelka *et al.*,

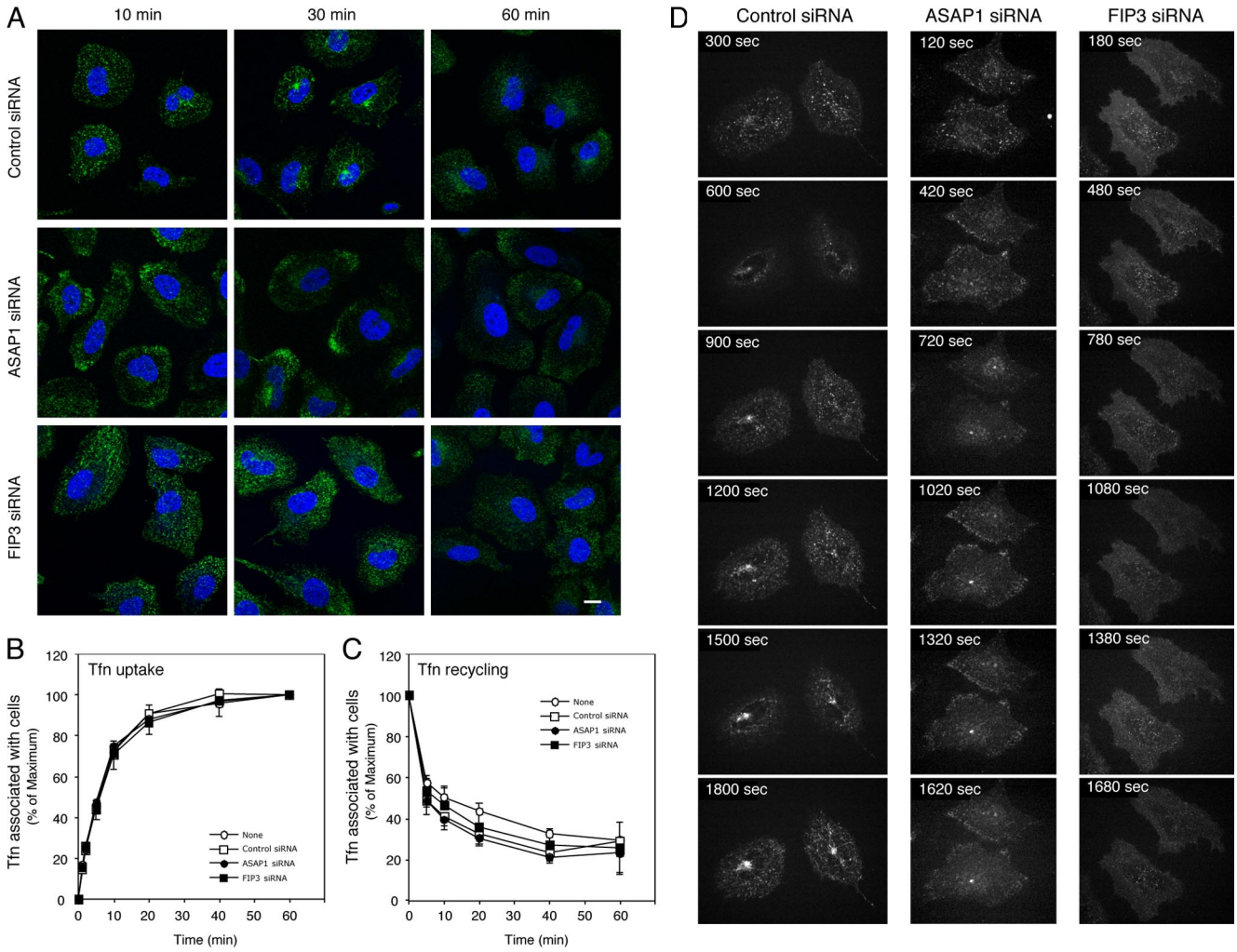

Figure 8. Depletion of ASAP1 or FIP3 alters the distribution of endocytosed transferrin, but does not affect the rate of either uptake or recycling. (A) Depletion of ASAP1 or FIP3 inhibits perinuclear accumulation of endocytosed Tfn. ASAP1- or FIP3-depleted HeLa cells were starved for 2 h, incubated with 50 μg/ml Alexa488-Tfn for 1 h on ice, washed with ice-cold medium to remove unbound Tfn, and allowed endocytosis and recycling of the labeled Tfn by warming up to 37°C. At the indicated time points, the cells were fixed, stained with Hoechst 33342, mounted, and then observed under microscope as in Figure 6. Bar, 10 μm. (B and C) Depletion of neither ASAP1 nor FIP3 affects the kinetics of Tfn uptake or recycling. The depleted cells were serum-starved for 2 h. In uptake experiments (B), the cells were incubated with 50 μg/ml biotin-Tfn for the indicated time at 37°C. To stop the reaction the cells were chilled on ice, washed with acid wash buffer (see *Materials and Methods*), and fixed with formaldehyde. After permeabilization with 0.1% Triton X-100, endocytosed biotin-Tfn was detected with HRP-labeled streptavidin and ABTS substrate and quantified with a microplate reader. In recycling experiments (C), the cells were incubated for 1 h with biotin-Tfn, washed with acid wash buffer, and incubated again for the indicated time without the labeled-Tfn. Thereafter, the reaction was stopped and the biotin-Tfn associated with the cells was detected as in B. (D) Live cell imaging of Tfn trafficking in ASAP1- or FIP3-depleted cells. The depleted HeLa cells were seeded on fibronectin-coated chambered cover glass and starved for 2 h. Alexa488-Tfn, 150 μg/ml, was bound to the cells in ice-cold serum-free medium for 1 h. After washing unbound Tfn, cells were warmed up to 37°C on UltraView spinning disk confocal microscope system equipped with a environmental chamber, and intracellular trafficking of the labeled Tfn was captured for 30 min. Selected frames from the movies (See Supplemental Materials) were shown about every 5 min.

2004; Caswell and Norman, 2006). In addition, Arf1 also mediates paxillin recruitment to focal adhesions (Norman *et al.*, 1998). We have found that CIN85, a multidomain adaptor protein involved in Cbl-mediated down-regulation of EGFR, interacts with ASAP1, and overexpression of ASAP1 increases the recycling of EGFR in CHO cells (Kowanetz *et al.*, 2004). More recently, CIN85 has been reported to colocalize with ASAP1 in invadopodia, and the complex of ASAP1 and CIN85 has been proposed to positively regulate the invasive phenotype of breast cancer cells (Nam *et al.*, 2007). A plausible model explaining these results is that ASAP1 regulates the recycling of transmembrane protein, such as integrins.

The staining for FIP3 was variable. FIP3 associated with recycling endosomes, which are distributed as groups of small vesicles in the perinuclear region. In addition, FIP3 also associated with single puncta in the pericentrosomal region in some cells. ASAP1 and FIP3 colocalize at the structure. The reason for the variable localization of FIP3 is not known, but may be related to the cell cycle as shown in *Drosophila* Nuf, orthologue of mammalian FIP3 and FIP4 (Rothwell *et al.*, 1998; Riggs *et al.*, 2003). Nuf is diffusely distributed in cells during interphase in *Drosophila* embryo, but accumulates in the pericentrosomal area during prophase before nuclear membrane breakdown. During metaphase to telophase, Nuf disappears from the region,

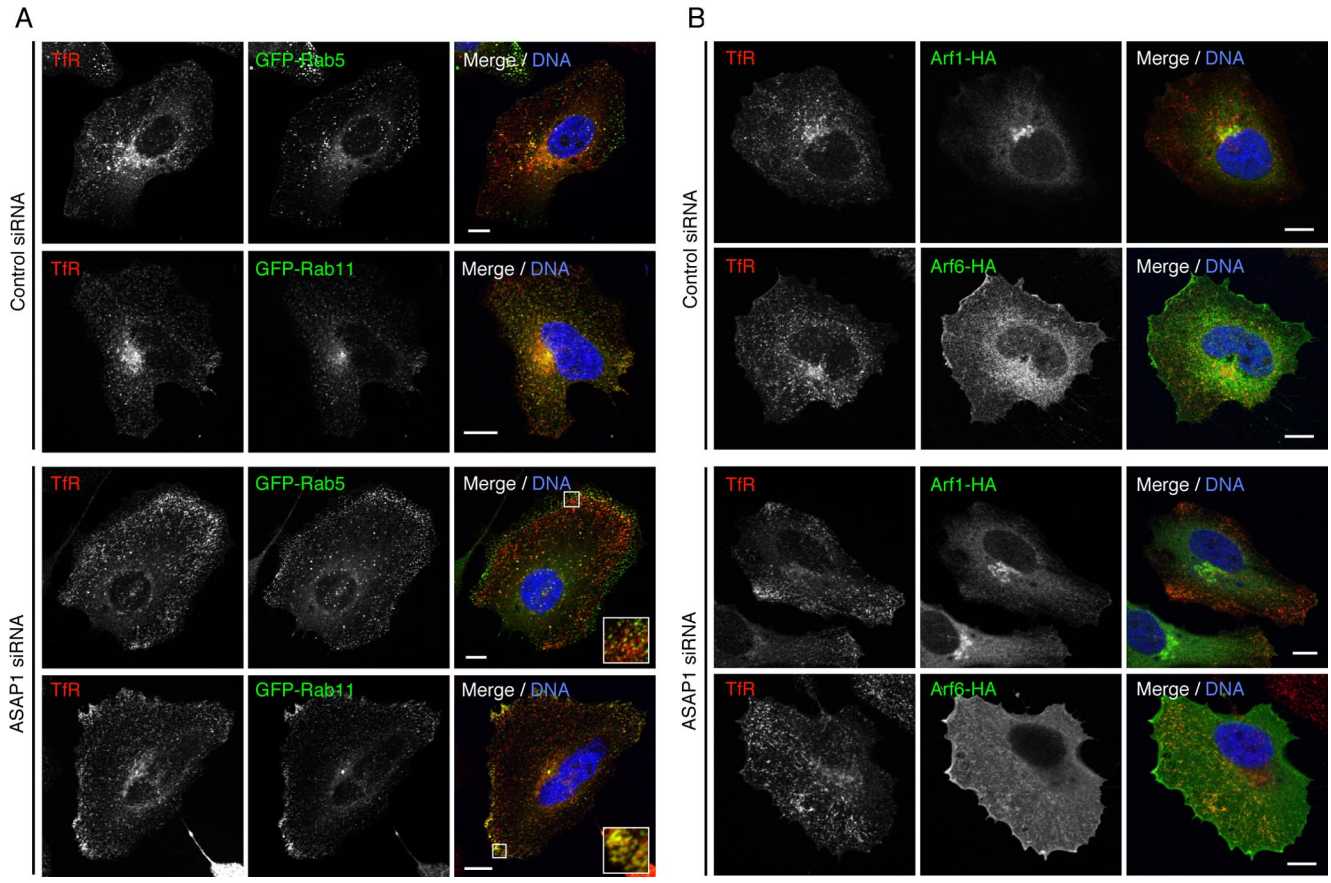

Figure 9. The peripheral TfR-positive endosomes induced by ASAP1 depletion contain Rab11, Arf1, and Arf6. (A) The peripheral TfR vesicles in ASAP1-depleted cell contain GFP-Rab11 but not GFP-Rab5. HeLa cells were transfected with siRNA for nontargeted control or ASAP1 and, after 48 h were transfected again with the expression vector for GFP-Rab5 or Rab11. Then, cells were seeded on fibronectin-coated cover glass and cultured overnight. Cells were fixed with formaldehyde and stained with anti-TfR antibody and Hoechst 33342. Images were taken as described in Figure 6. (B) ASAP1 depletion affects the cellular distribution of Arf1-HA and Arf6-HA. HeLa cells were transfected with siRNA and plasmid DNA for Arf1-HA or Arf6-HA, seeded on a cover glass, fixed, stained, and visualized as described in A. Bar, 10 μm.

and accumulates again during cellularization, which corresponds to cytokinesis in mammalian cells.

Part of the variability in FIP3 localization could be related to having more than one binding partner responsible for

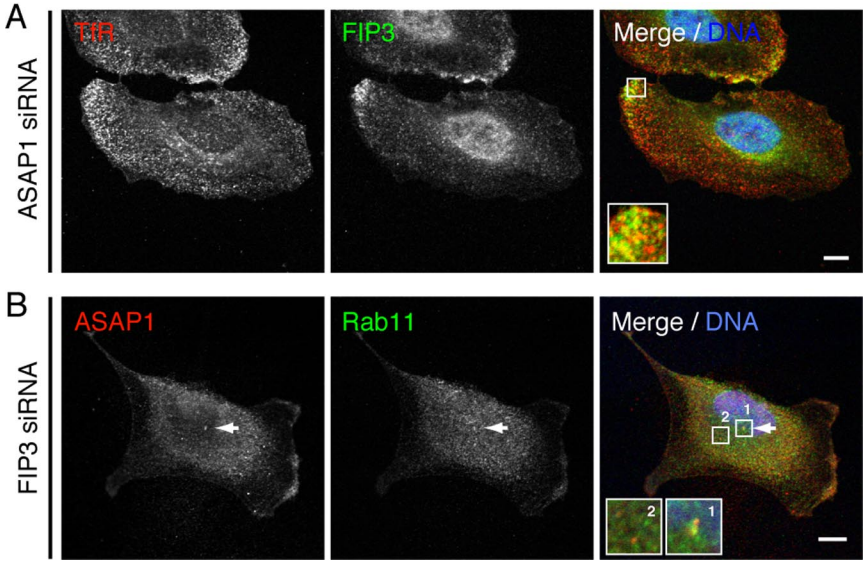

Figure 10. Effect of ASAP1 depletion on FIP3 distribution and FIP3 depletion on ASAP1 distribution. HeLa cells were transfected with siRNA for ASAP1 (A) or FIP3 (B), and 48 h after transfection the cells were spread on fibronectin-coated cover glass. Seventy-two hours after transfection, cells were fixed with cold methanol and then stained with indicated antibodies and Hoechst33342. Boxed areas are enlarged as insets. Perinuclear localization of ASAP1 in B is indicated with arrow. Bar, 10 μm.

localization. FIP3 localizes at recycling endosomes in a Rab11-dependent manner (Horgan *et al.*, 2007). We found that association of FIP3 with the perinuclear puncta depends on ASAP1 expression, whereas association of ASAP1 with the puncta does not depend on FIP3. On the basis of this result and the finding that FIP3 binds to ASAP1, we propose that FIP3 is recruited to the perinuclear puncta by ASAP1. The mechanism by which ASAP1 associates with this structure remains to be defined.

We found that depletion of ASAP1 using siRNA in HeLa cells perturbs perinuclear localization of Tfn and TfR and induces their accumulation at the cell edge in a compartment that contains Rab11 and FIP3. Despite the significant change of the localization of Tfn and TfR, the kinetics of Tfn internalization and recycling were not affected. There are other examples of changes in the distribution of perinuclear recycling endosome that do not affect the kinetics of Tfn recycling; overexpression of FIP3 or FIP4 induces accumulation of perinuclear recycling endosomes, but there is no effect on Tfn recycling rate (Hickson *et al.*, 2003; Horgan *et al.*, 2004). Similarly, siRNA-mediated depletion of annexin 2, a Ca^{2+}-dependent endosome membrane-associated protein, causes accumulation of recycling endosomes in the perinuclear region, but has no significant effect on the rate of recycling (Zobiack *et al.*, 2003). Taken together, we conclude that the kinetics of Tfn recycling do not depend on proper positioning of the perinuclear recycling endosomes, although we cannot exclude that alternative pathways for internalization and recycling may compensate for a defect derived from single protein. Because TfR recycling can occur through either the sorting endosome or the recycling endosome and the depletion of ASAP1 does not appear to affect the sorting endosome, as marked by Rab5, Tfn recycling is likely intact because transport through the sorting endosome still occurs. This idea is also supported by the live-cell tracking of Tfn.

The peripheral vesicles observed when ASAP1 was depleted contained TfR, Tfn, Rab11, and FIP3, typical recycling endosome marker. We concluded that the vesicles were recycling endosomes that were displaced from the usual perinuclear localization. We also analyzed the localization of Arf1 and Arf6 in the cells. In control siRNA-transfected cells, we detected that a small amount of Arf1 and Arf6 on TfR-positive vesicles at perinuclear region, which becomes reduced upon the depletion of ASAP1. Because AP-1 and Arf guanine nucleotide exchange factor BIG2 act at the recycling endosome in addition to the TGN (Deneka *et al.*, 2003; Shin *et al.*, 2004), Arf1 as well as Arf6 may be involved in the function of the recycling endosome. In this context, ASAP1 may regulate Arf1 association to the recycling endosome and, as a consequence, the translocation of the endosomes from the pericentrosomal region to the cell periphery.

In summary, our data support the conclusion that the BAR domain of ASAP1 interacts with the coiled-coil region of FIP3, and the binding stimulates ASAP1 Arf GAP activity. Both FIP3 and ASAP1 are required for proper localization of the perinuclear endocytic recycling compartment containing Tfn and TfR. These findings provided new insights into the nature of BAR domains as protein-interacting module and the function of ASAP1 on membrane trafficking. We also propose that FIP3 functions as a novel coat protein because it associates with Arfs and Arf GAP and regulates the GAP activity, which are properties of other coat proteins including COPs, APs, and GGAs.

ACKNOWLEDGMENTS

We thank Drs. Gwyn W. Gould (University of Glasgow, Scotland), Julie G. Donaldson (National Heart, Lung, and Blood Institute, Bethesda, MD), Roberto Weigert (National Institute of Dental and Craniofacial Research, Bethesda, MD), and Yoshiyuki Wakabayashi (National Institute of Child Health and Human Development, Bethesda, MD) for reagents. We also thank Drs. Susan Garfield and Valarie Barr (National Cancer Institute, Bethesda, MD) for technical assistance with confocal microscopy. This work was supported by the Intramural Research Program of the National Cancer Institute, Department of Health and Human Services.

REFERENCES

Bharti, S. *et al.* (2007). Src-dependent phosphorylation of ASAP1 regulates podosomes. Mol. Cell. Biol. *27*, 8271–8283.

Brown, F. D., Rozelle, A. L., Yin, H. L., Balla, T., and Donaldson, J. G. (2001). Phosphatidylinositol 4,5-bisphosphate and Arf6-regulated membrane traffic. J. Cell Biol. *154*, 1007–1017.

Brown, M. T., Andrade, J., Radhakrishna, H., Donaldson, J. G., Cooper, J. A., and Randazzo, P. A. (1998). ASAP1, a phospholipid-dependent arf GTPase-activating protein that associates with and is phosphorylated by Src. Mol. Cell. Biol. *18*, 7038–7051.

Buccione, R., Orth, J. D., and McNiven, M. A. (2004). Foot and mouth: podosomes, invadopodia and circular dorsal ruffles. Nat. Rev. Mol. Cell Biol. *5*, 647–657.

Carlton, J., Bujny, M., Peter, B. J., Oorschot, V. M., Rutherford, A., Mellor, H., Klumperman, J., McMahon, H. T., and Cullen, P. J. (2004). Sorting nexin-1 mediates tubular endosome-to-TGN transport through coincidence sensing of high-curvature membranes and 3-phosphoinositides. Curr. Biol. *14*, 1791–1800.

Caswell, P. T., and Norman, J. C. (2006). Integrin trafficking and the control of cell migration. Traffic *7*, 14–21.

Che, M. M., Boja, E. S., Yoon, H. Y., Gruschus, J., Jaffe, H., Stauffer, S., Schuck, P., Fales, H. M., and Randazzo, P. A. (2005a). Regulation of ASAP1 by phospholipids is dependent on the interface between the PH and Arf GAP domains. Cell Signal. *17*, 1276–1288.

Che, M. M., Nie, Z., and Randazzo, P. A. (2005b). Assays and properties of the Arf GAPs AGAP1, ASAP1, and Arf GAP1. Methods Enzymol. *404*, 147–163.

Cohen, L. A., Honda, A., Varnai, P., Brown, F. D., Balla, T., and Donaldson, J. G. (2007). Active Arf6 recruits ARNO/cytohesin GEFs to the PM by binding their PH domains. Mol. Biol. Cell *18*, 2244–2253.

Deneka, M., Neeft, M., Popa, I., van Oort, M., Sprong, H., Oorschot, V., Klumperman, J., Schu, P., and van der Sluijs, P. (2003). Rabaptin-5alpha/rabaptin-4 serves as a linker between rab4 and gamma(1)-adaptin in membrane recycling from endosomes. EMBO J. *22*, 2645–2657.

D'Souza-Schorey, C., and Chavrier, P. (2006). ARF proteins: roles in membrane traffic and beyond. Nat. Rev. Mol. Cell Biol. *7*, 347–358.

Eathiraj, S., Mishra, A., Prekeris, R., and Lambright, D. G. (2006). Structural basis for Rab11-mediated recruitment of FIP3 to recycling endosomes. J. Mol. Biol. *364*, 121–135.

Fielding, A. B., Schonteich, E., Matheson, J., Wilson, G., Yu, X., Hickson, G. R., Srivastava, S., Baldwin, S. A., Prekeris, R., and Gould, G. W. (2005). Rab11-FIP3 and FIP4 interact with Arf6 and the exocyst to control membrane traffic in cytokinesis. EMBO J. *24*, 3389–3399.

Furman, C., Short, S. M., Subramanian, R. R., Zetter, B. R., and Roberts, T. M. (2002). DEF-1/ASAP1 is a GTPase-activating protein (GAP) for ARF1 that enhances cell motility through a GAP-dependent mechanism. J. Biol. Chem. *277*, 7962–7969.

Fütterer, K., and Machesky, L. M. (2007). "Wunder" F-BAR domains: going from pits to vesicles. Cell *129*, 655–657.

Gillingham, A. K., and Munro, S. (2007). The small G proteins of the Arf family and their regulators. Annu. Rev. Cell Dev. Biol. *23*, 579–611.

Ha, V. L., Bharti, S., Inoue, H., Vass, W. C., Campa, F., Nie, Z., de Gramont, A., Ward, Y., and Randazzo, P. A. (2008). ASAP3 is a focal adhesion-associated Arf GAP that functions in cell migration and invasion. J. Biol. Chem. *283*, 14915–14926.

Habermann, B. (2004). The BAR-domain family of proteins: a case of bending and binding? EMBO Rep. *5*, 250–255.

Hashimoto, S., Hashimoto, A., Yamada, A., Kojima, C., Yamamoto, H., Tsutsumi, T., Higashi, M., Mizoguchi, A., Yagi, R., and Sabe, H. (2004). A novel mode of action of an ArfGAP, AMAP2/PAG3/Pap alpha, in Arf6 function. J. Biol. Chem. *279*, 37677–37684.

Haucke, V. (2005). Phosphoinositide regulation of clathrin-mediated endocytosis. Biochem. Soc. Trans. *33*, 1285–1289.

Hickson, G. R., Matheson, J., Riggs, B., Maier, V. H., Fielding, A. B., Prekeris, R., Sullivan, W., Barr, F. A., and Gould, G. W. (2003). Arfophilins are dual Arf/Rab 11 binding proteins that regulate recycling endosome distribution and are related to *Drosophila* nuclear fallout. Mol. Biol. Cell *14*, 2908–2920.

Horgan, C. P., Oleksy, A., Zhdanov, A. V., Lall, P. Y., White, I. J., Khan, A. R., Futter, C. E., McCaffrey, J. G., and McCaffrey, M. W. (2007). Rab11-FIP3 is critical for the structural integrity of the endosomal recycling compartment. Traffic *8*, 414–430.

Horgan, C. P., Walsh, M., Zurawski, T. H., and McCaffrey, M. W. (2004). Rab11-FIP3 localises to a Rab11-positive pericentrosomal compartment during interphase and to the cleavage furrow during cytokinesis. Biochem. Biophys. Res. Commun. *319*, 83–94.

Inoue, H., and Randazzo, P. A. (2007). Arf GAPs and their interacting proteins. Traffic *8*, 1465–1475.

Jackson, T. R., Brown, F. D., Nie, Z., Miura, K., Foroni, L., Sun, J., Hsu, V. W., Donaldson, J. G., and Randazzo, P. A. (2000). ACAPs are arf6 GTPase-activating proteins that function in the cell periphery. J. Cell Biol. *151*, 627–638.

Kam, J. L., Miura, K., Jackson, T. R., Gruschus, J., Roller, P., Stauffer, S., Clark, J., Aneja, R., and Randazzo, P. A. (2000). Phosphoinositide-dependent activation of the ADP-ribosylation factor GTPase-activating protein ASAP1. Evidence for the pleckstrin homology domain functioning as an allosteric site. J. Biol. Chem. *275*, 9653–9663.

Kowanetz, K. *et al*. (2004). CIN85 associates with multiple effectors controlling intracellular trafficking of epidermal growth factor receptors. Mol. Biol. Cell *15*, 3155–3166.

Kumari, S., and Mayor, S. (2008). ARF1 is directly involved in dynamin-independent endocytosis. Nat. Cell Biol. *10*, 30–41.

Lee, E., Marcucci, M., Daniell, L., Pypaert, M., Weisz, O. A., Ochoa, G. C., Farsad, K., Wenk, M. R., and De Camilli, P. (2002). Amphiphysin 2 (Bin1) and T-tubule biogenesis in muscle. Science *297*, 1193–1196.

Liu, Y., Loijens, J. C., Martin, K. H., Karginov, A. V., and Parsons, J. T. (2002). The association of ASAP1, an ADP ribosylation factor-GTPase activating protein, with focal adhesion kinase contributes to the process of focal adhesion assembly. Mol. Biol. Cell *13*, 2147–2156.

Liu, Y., Yerushalmi, G. M., Grigera, P. R., and Parsons, J. T. (2005). Mislocalization or reduced expression of Arf GTPase-activating protein ASAP1 inhibits cell spreading and migration by influencing Arf1 GTPase cycling. J. Biol. Chem. *280*, 8884–8892.

Masuda, M., Takeda, S., Sone, M., Ohki, T., Mori, H., Kamioka, Y., and Mochizuki, N. (2006). Endophilin BAR domain drives membrane curvature by two newly identified structure-based mechanisms. EMBO J. *25*, 2889–2897.

Miaczynska, M., Christoforidis, S., Giner, A., Shevchenko, A., Uttenweiler-Joseph, S., Habermann, B., Wilm, M., Parton, R. G., and Zerial, M. (2004). APPL proteins link Rab5 to nuclear signal transduction via an endosomal compartment. Cell *116*, 445–456.

Nam, J. M., Onodera, Y., Mazaki, Y., Miyoshi, H., Hashimoto, S., and Sabe, H. (2007). CIN85, a Cbl-interacting protein, is a component of AMAP1-mediated breast cancer invasion machinery. EMBO J. *26*, 647–656.

Nie, Z. *et al.* (2006). A BAR domain in the N terminus of the Arf GAP ASAP1 affects membrane structure and trafficking of epidermal growth factor receptor. Curr. Biol. *16*, 130–139.

Norman, J. C., Jones, D., Barry, S. T., Holt, M. R., Cockcroft, S., and Critchley, D. R. (1998). ARF1 mediates paxillin recruitment to focal adhesions and potentiates Rho-stimulated stress fiber formation in intact and permeabilized Swiss 3T3 fibroblasts. J. Cell Biol. *143*, 1981–1995.

Oda, A. *et al.* (2003). CrkL directs ASAP1 to peripheral focal adhesions. J. Biol. Chem. *278*, 6456–6460.

Onodera, Y. *et al.* (2005). Expression of AMAP1, an ArfGAP, provides novel targets to inhibit breast cancer invasive activities. EMBO J. *24*, 963–973.

Pagano, A., Crottet, P., Prescianotto-Baschong, C., and Spiess, M. (2004). In vitro formation of recycling vesicles from endosomes requires adaptor protein-1/clathrin and is regulated by rab4 and the connector rabaptin-5. Mol. Biol. Cell *15*, 4990–5000.

Peter, B. J., Kent, H. M., Mills, I. G., Vallis, Y., Butler, P. J., Evans, P. R., and McMahon, H. T. (2004). BAR domains as sensors of membrane curvature: the amphiphysin BAR structure. Science *303*, 495–499.

Powelka, A. M., Sun, J., Li, J., Gao, M., Shaw, L. M., Sonnenberg, A., and Hsu, V. W. (2004). Stimulation-dependent recycling of integrin beta1 regulated by ARF6 and Rab11. Traffic *5*, 20–36.

Prekeris, R. (2003). Rabs, Rips, FIPs, and endocytic membrane traffic. Sci. World J. *3*, 870–880.

Prekeris, R, Davies, J. M., and Scheller, R. H. Identification of a novel Rab11/25 binding domain present in Eferin and Rip proteins. J. Biol. Chem. (2001). *276*, 38966–38970.

Randazzo, P. A., Andrade, J., Miura, K., Brown, M. T., Long, Y. Q., Stauffer, S., Roller, P., and Cooper, J. A. (2000). The Arf GTPase-activating protein ASAP1 regulates the actin cytoskeleton. Proc. Natl. Acad. Sci. USA *97*, 4011–4016.

Randazzo, P. A., Inoue, H., and Bharti, S. (2007). Arf GAPs as regulators of the actin cytoskeleton. Biol. Cell *99*, 583–600.

Riggs, B., Rothwell, W., Mische, S., Hickson, G. R., Matheson, J., Hays, T. S., Gould, G. W., and Sullivan, W. (2003). Actin cytoskeleton remodeling during early *Drosophila* furrow formation requires recycling endosomal components Nuclear-fallout and Rab11. J. Cell Biol. *163*, 143–154.

Rothwell, W. F., Fogarty, P., Field, C. M., and Sullivan, W. (1998). Nuclear-fallout, a *Drosophila* protein that cycles from the cytoplasm to the centrosomes, regulates cortical microfilament organization. Development *125*, 1295–1303.

Santy, L. C., and Casanova, J. E. (2001). Activation of ARF6 by ARNO stimulates epithelial cell migration through downstream activation of both Rac1 and phospholipase D. J. Cell Biol. *154*, 599–610.

Schonteich, E., Pilli, M., Simon, G. C., Matern, H. T., Junutula, J. R., Sentz, D., Holmes, R. K., and Prekeris, R. (2007). Molecular characterization of Rab11-FIP3 binding to ARF GTPases. Eur. J. Cell Biol. *86*, 417–431.

Shiba, T., Koga, H., Shin, H. W., Kawasaki, M., Kato, R., Nakayama, K., and Wakatsuki, S. (2006). Structural basis for Rab11-dependent membrane recruitment of a family of Rab11-interacting protein 3 (FIP3)/Arfophilin-1. Proc. Natl. Acad. Sci. USA *103*, 15416–15421.

Shin, H. W., Morinaga, N., Noda, M., and Nakayama, K. (2004). BIG2, a guanine nucleotide exchange factor for ADP-ribosylation factors: its localization to recycling endosomes and implication in the endosome integrity. Mol. Biol. Cell *15*, 5283–5294.

Shin, O. H., Couvillon, A. D., and Exton, J. H. (2001). Arfophilin is a common target of both class II and class III ADP-ribosylation factors. Biochemistry *40*, 10846–10852.

Shin, O. H., Ross, A. H., Mihai, I., and Exton, J. H. (1999). Identification of arfophilin, a target protein for GTP-bound class II ADP-ribosylation factors. J. Biol. Chem. *274*, 36609–36615.

Sintchak, M. D., Fleming, M. A., Futer, O., Raybuck, S. A., Chambers, S. P., Caron, P. R., Murcko, M. A., and Wilson, K. P. (1996). Structure and mechanism of inosine monophosphate dehydrogenase in complex with the immunosuppressant mycophenolic acid. Cell *85*, 921–930.

Takei, K., Slepnev, V. I., Haucke, V., and De Camilli, P. (1999). Functional partnership between amphiphysin and dynamin in clathrin-mediated endocytosis. Nat. Cell Biol. *1*, 33–39.

Tarricone, C., Xiao, B., Justin, N., Walker, P. A., Rittinger, K., Gamblin, S. J., and Smerdon, S. J. (2001). The structural basis of Arfaptin-mediated cross-talk between Rac and Arf signalling pathways. Nature *411*, 215–219.

van IJzendoorn, S. C. (2006). Recycling endosomes. J. Cell Sci. *119*, 1679–1681.

Wallace, D. M., Lindsay, A. J., Hendrick, A. G., and McCaffrey, M. W. (2002). The novel Rab11-FIP/Rip/RCP family of proteins displays extensive homo- and hetero-interacting abilities. Biochem. Biophys. Res. Commun. *292*, 909–915.

Wilson, G. M., Fielding, A. B., Simon, G. C., Yu, X., Andrews, P. D., Hames, R. S., Frey, A. M., Peden, A. A., Gould, G. W., and Prekeris, R. (2005). The FIP3-Rab11 protein complex regulates recycling endosome targeting to the cleavage furrow during late cytokinesis. Mol. Biol. Cell *16*, 849–860.

Zerial, M., and McBride, H. (2001). Rab proteins as membrane organizers. Nat. Rev. Mol. Cell Biol. *2*, 107–117.

Zhu, G., Chen, J., Liu, J., Brunzelle, J. S., Huang, B., Wakeham, N., Terzyan, S., Li, X., Rao, Z., Li, G., and Zhang, X. C. (2007). Structure of the APPL1 BAR-PH domain and characterization of its interaction with Rab5. EMBO J. *26*, 3484–3493.

Zobiack, N., Rescher, U., Ludwig, C., Zeuschner, D., and Gerke, V. (2003). The annexin 2/S100A10 complex controls the distribution of transferrin receptor-containing recycling endosomes. Mol. Biol. Cell *14*, 4896–4908.